Fermi National Accelerator Laboratory

FN-331
1620.000

PROPERTIES OF SUPERCONDUCTING MAGNETS*

A. V. Tollestrup

July 21, 1980

(Talk given at March Brookhaven National Laboratory Workshop on Superconducting Accelerator Magnets)

Operated by Universities Research Association Inc. under contract with the United States Department of Energy

Preparing for this talk has been an interesting experience. I have had a chance to go back and review many of our early data books, and it has become clear that in the last 5 years, while we have advanced from making 1 ft. magnets to making 22 ft. magnets, there are still many questions concerning superconducting magnet technology that remain unanswered. In some areas such as systems, quality control, vacuum technology, and cryostat construction, we have made great strides. In other areas such as understanding why magnets train, we have made very little progress. The data I will use in this talk will mostly be taken from Fermilab sources, and it involves the work of many people that have been in the program since its inception. From what I have seen and heard, similar data has been accumulated by workers at other laboratories. Now let's look at the data:

Training

Perhaps one of the most unique features of superconducting magnets is the fact that they "train." Projection 1 shows the training curves of 4 different magnets. By training, we mean the phenomena that as the current is ramped up in a new magnet, it will reach a point at which a section of the superconductor goes normal. At this point, some means must be found to reduce the current to zero or the conductor will melt. The next time the current is run up, the magnet will go to a slightly higher field. A good example of this is shown for Magnet E10-1A. A magnet such as this would not be suitable for use in an accelerator. The other 3 magnets shown in the projection have somewhat better training characteristics. An example of a very

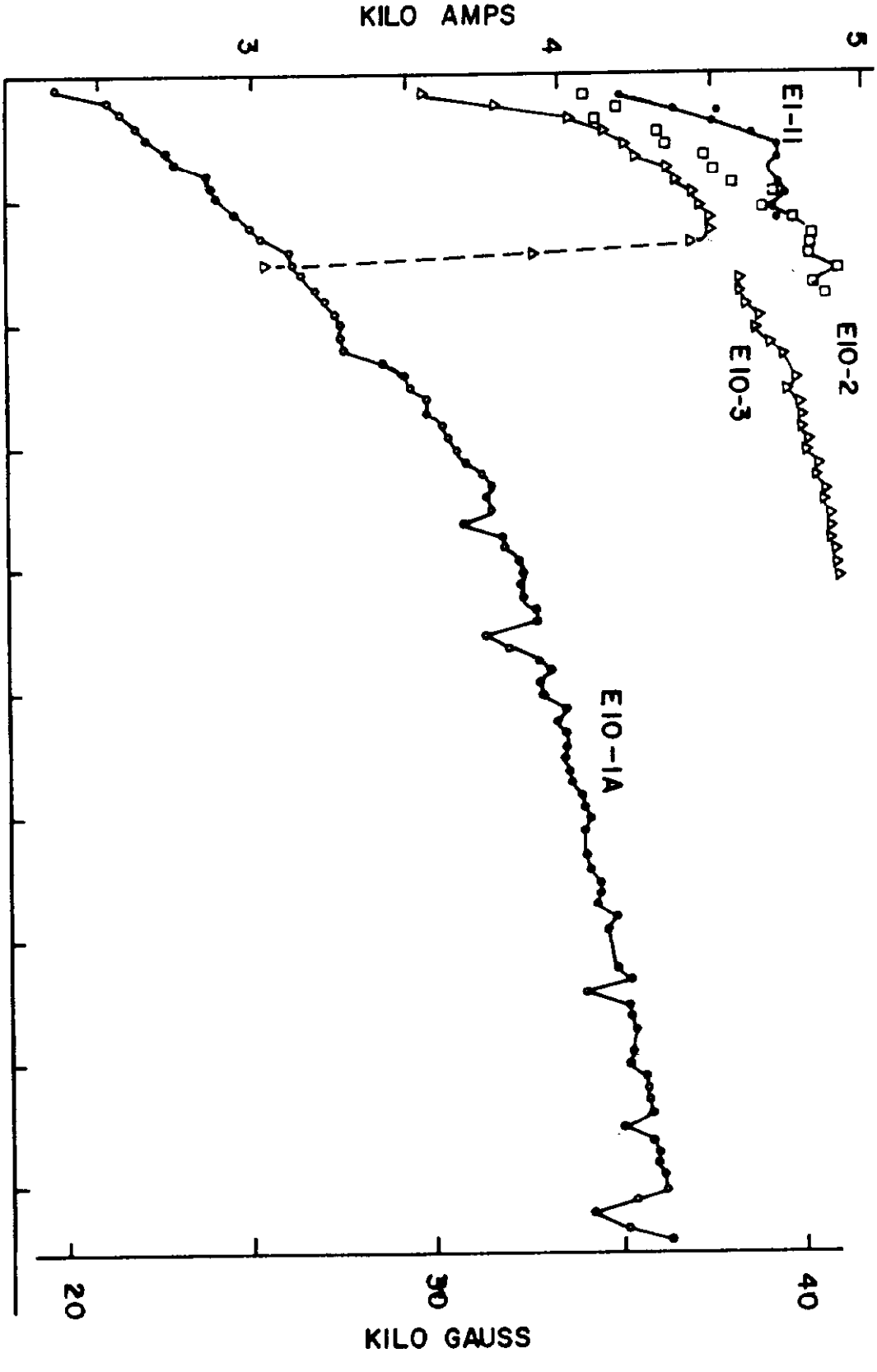

TRAINING CURVES
10' E SERIES

Projection 1

well behaved magnet is shown in Projection 2, where it is clear that the magnet is essentially fully trained after the first quench. The falling points after the second quench is because the magnet was tested at a high $\dot{B}$ and should be disregarded for this part of our discussion. This particular magnet PAB-59 reached a current of 5,150 amps, which represents the short sample limit of the conductor used in the construction of the magnet. If a magnet quenches before it has reached the short sample limit, it necessarily follows that some portion of the conductor went normal during the ramp. This section of the talk will concern itself with the differences between magnets like E10-1A and PAB-59.

Projection 3 shows a histogram of the number of quenches necessary to reach 95 percent of I_{max} for a series of magnets that were constructed early in the Fermilab program. It is seen from this histogram that it is possible to build magnets that behave in a fashion suitable for use in an accelerator. Projection 4 displays an additional aspect of this data, namely, it shows a histogram of the distribution of peak current in the magnet relative to the short sample limit of the wire of which the magnet was constructed. Projection 5 shows the histogram of the actual maximum quench current reached for the individual magnets.

It is clear that this data represents a series of magnets that trained with relatively few quenches to a current that approached very close to the short sample limit of the wire.

I would now like to address the question of what causes a magnet to quench before it reaches the short sample limit and why does a magnet train,

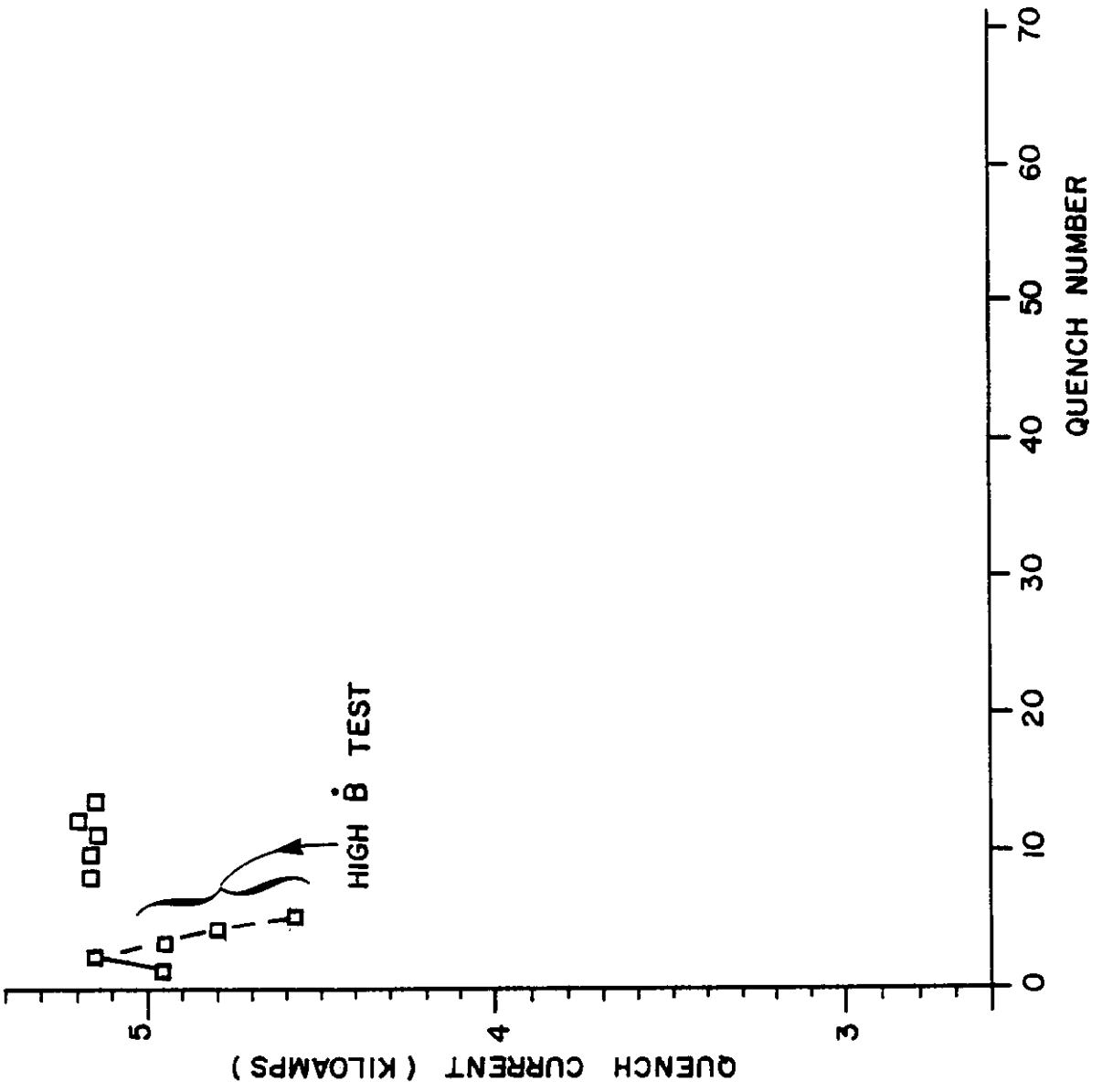

Projection 2

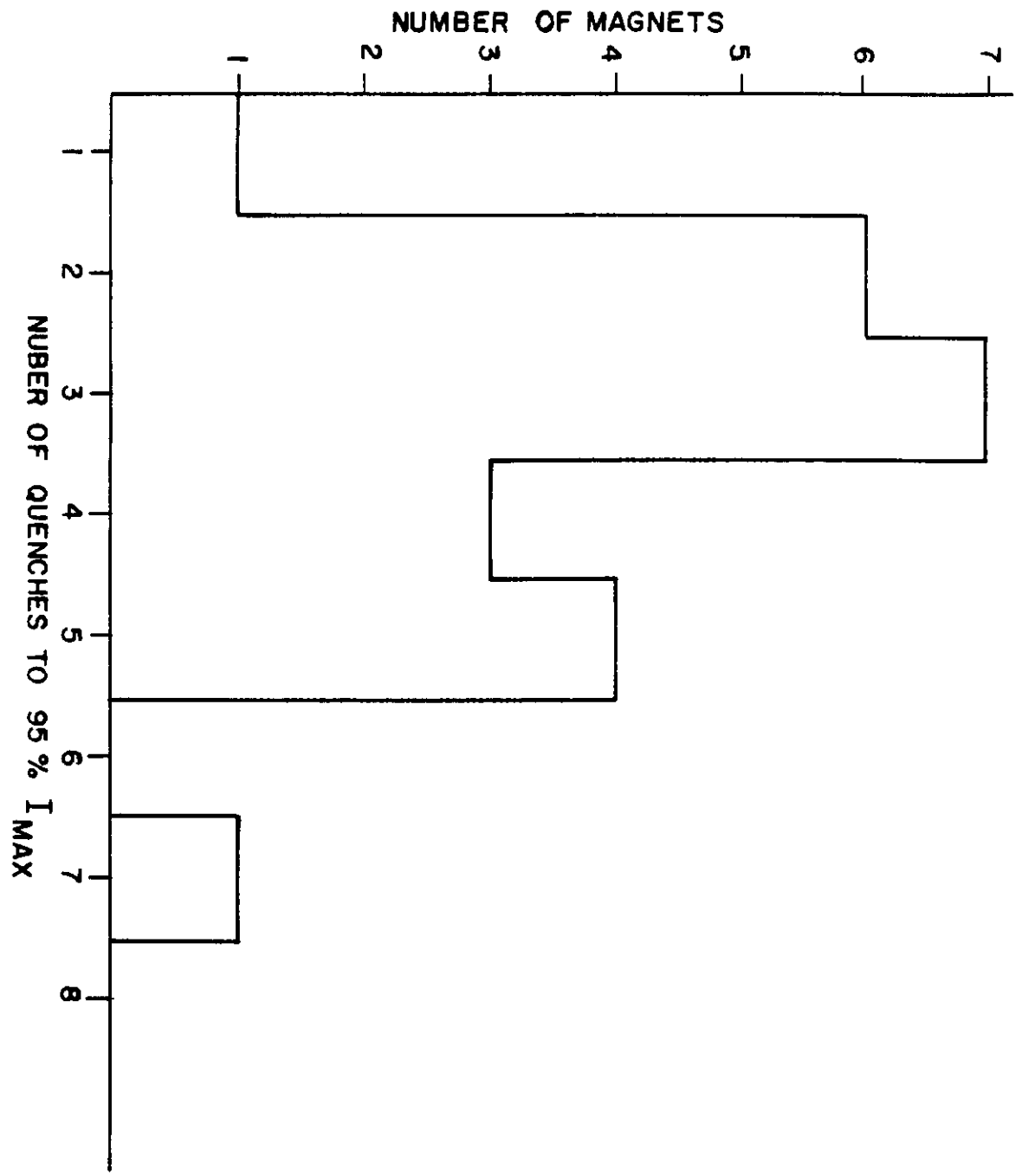

Projection 3

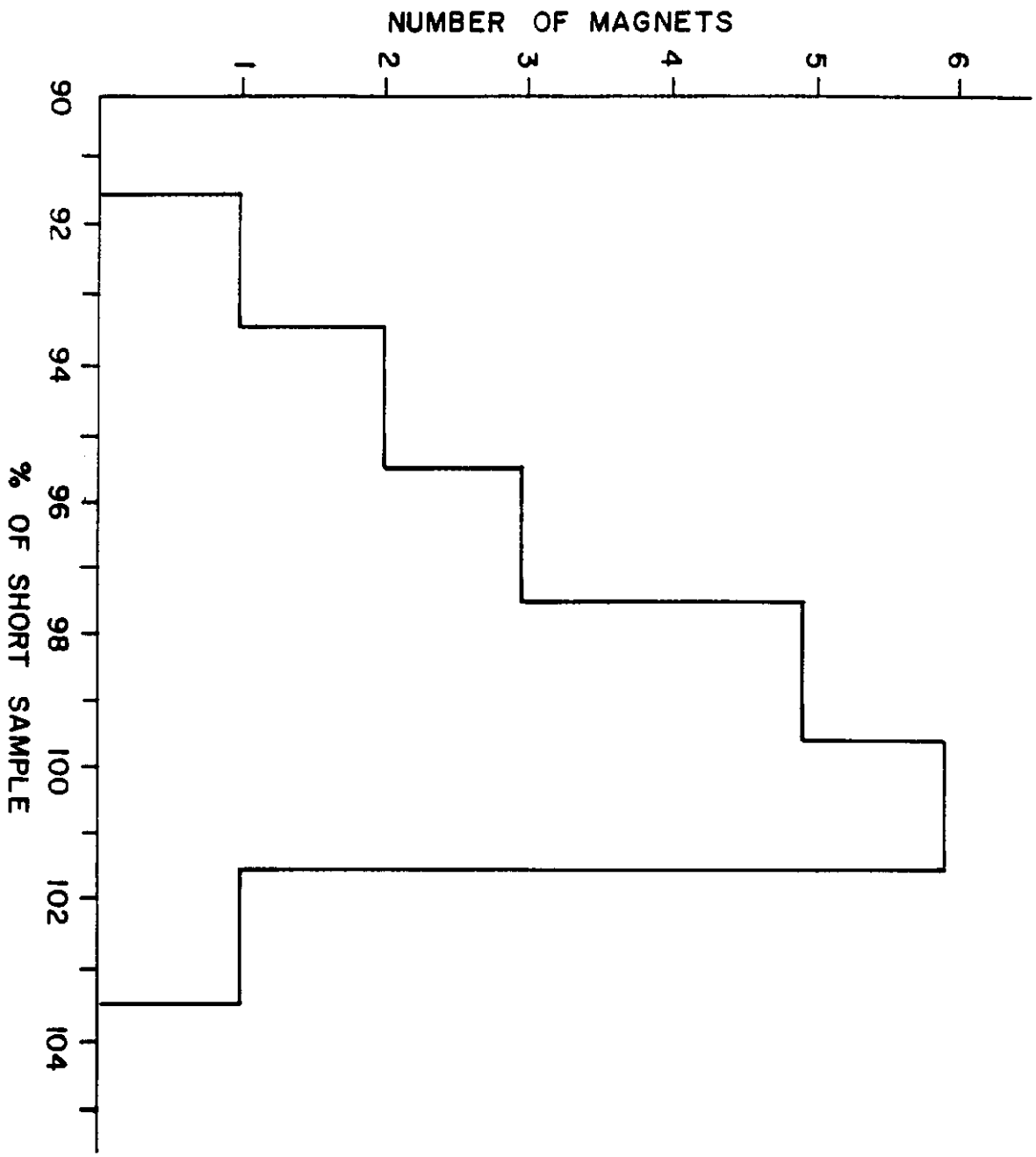

Projection 4

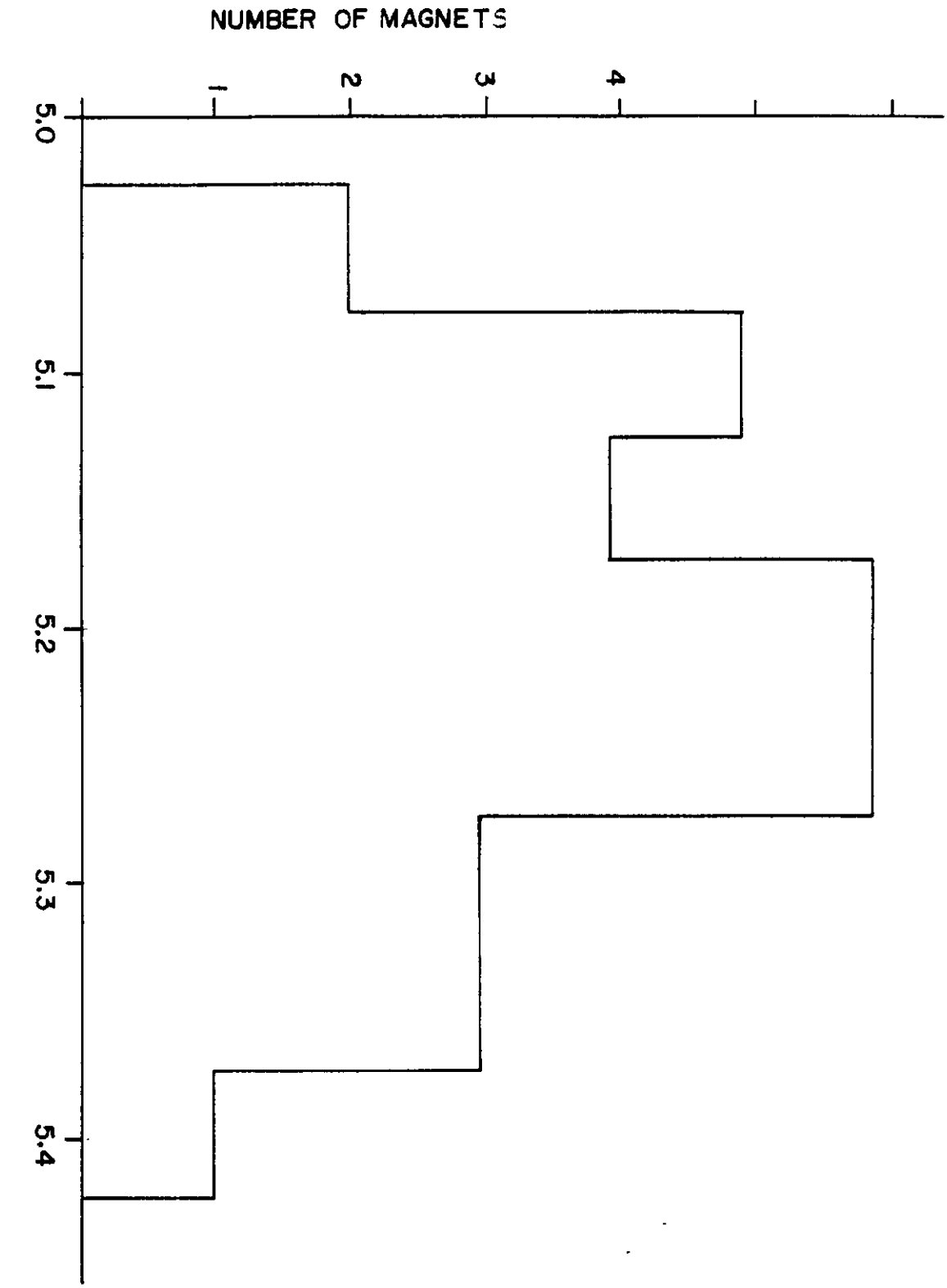

Projection 5

i.e., why does the current at which it quenches increase each time it is quenched? It is obvious that we would like to identify the mechanism for quenching and the mechanism for training.

In Projection 6, I show a number of quantities that I have calculated for a FNAL magnet. The horizontal scale represents temperature, and the vertical scale represents energy. The curve labeled cable enthalpy represents the total heat content of our 23 conductor wire as a function of temperature per centimeter of length of cable. It is seen that at 5^{o} K the energy content of the cable is less than a millijoule per centimeter of length. The slope of this curve at the operating temperature of 4.2^{o} K is about .2 mJ per degree K. The critical temperature for niobium titanium is around 10^{o} K, and hence, it would take about 4 mJ of energy per centimeter of cable in order to raise the temperature to the point where it would no longer be superconducting. However, when the cable is in a magnetic field and carrying a current, a much smaller change in temperature will drive the cable normal. For instance, if the cable is at 90 percent of the short sample limit, a change of a tenth of a degree K will change the cable from superconducting to normal. The $I^{2}r$ loss in the cable is then high enough to drive a quench wave down the conductor. We will discuss this phenomena in more detail later.

Thus, when we see a newly constructed magnet quenching at lower currents than the short sample limit, we are forced to look at sources of heat available for driving the wire normal and sources of cooling for absorbing such heat. There are two potential heat sinks available. The first is the specific heat of the matrix and any liquid helium contained around the wire. The Fermilab cable has a certain amount of open space available for helium

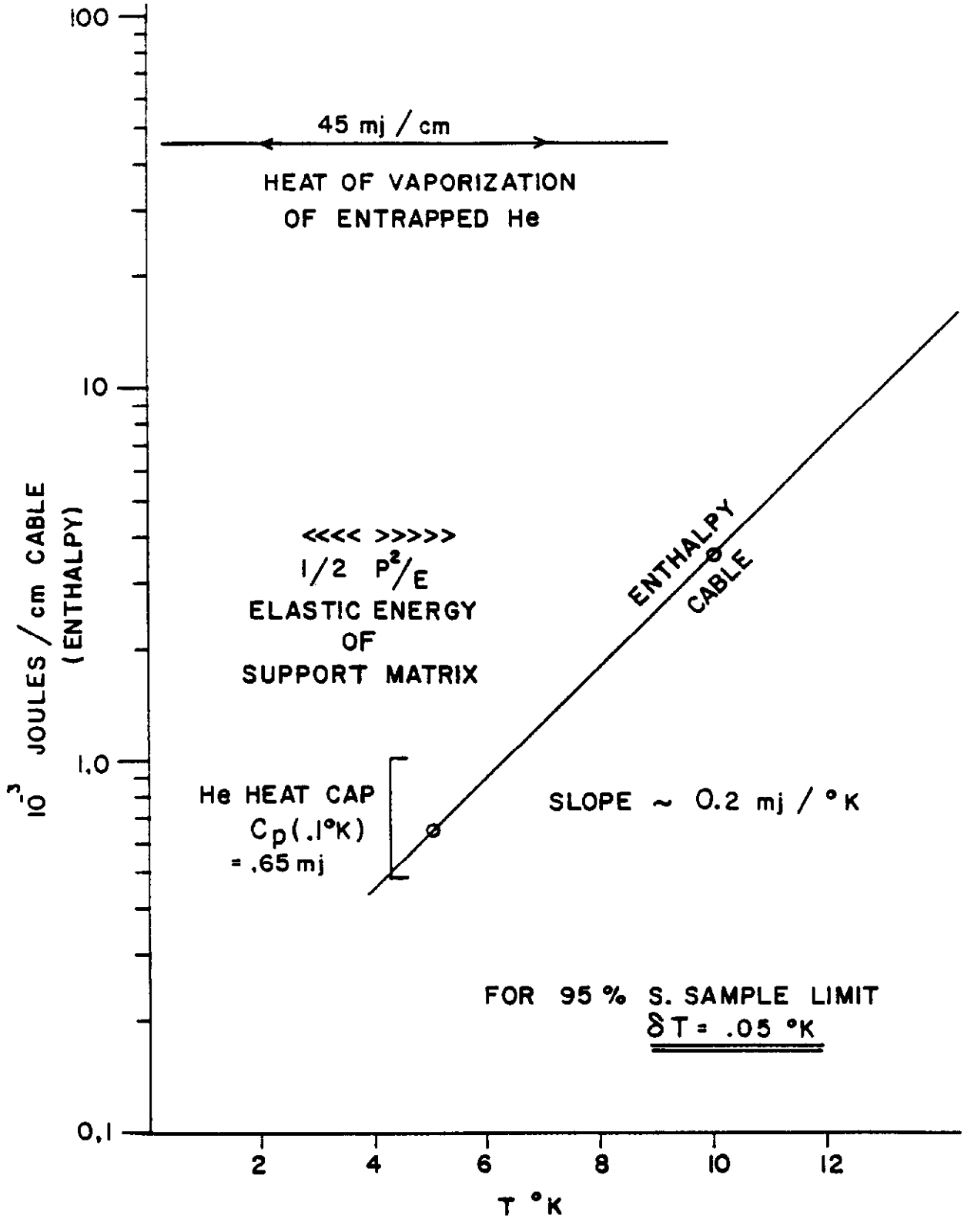

Projection 6

penetration. This amounts to about 10 percent of the cross section of the wire. I have shown on the curve the heat capacity of the captured liquid helium for a $1/10^{\circ}$ change in temperature (this assumes no boiling). It is equal to .65 mJ per centimeter of length of the wire. The ultimate heat capacity from this captured helium would be represented by the heat of vaporization, and that is shown by the arrow at the top of the graph, and it is 45 mJ per centimeter of length. It is thus clear that the helium represents the major heat sink in the magnet. To give some idea of the source of energy available for initiating a quench, I have shown $1/2\ P^2/E$, which is the elastic energy stored in the matrix. Again, I have normalized this to the volume of a centimeter length of the cable. The Youngs modulus used is $E = 10^6$ and is representative of the Fermilab design. P^2 is of the order of several thousand pounds per square inch. It is clear that the energy stored elastically is much bigger than the energy needed to drive the wire normal when it is carrying a current close to the short sample limit. However, I was surprised to see that this energy is not enormously large compared to the energy required to initiate a quench nor is it very large compared to the heat sink available in the helium.

It should be mentioned at this point that there are two prevalent theories concerning the source of the energy to initiate a quench below the short sample limit. The first involves frictional motion of the conductor under Lorentz forces, and the second theory postulates that the support matrix cracks under the strain of the Lorentz forces, and the strain energy is absorbed by the conductor and drives it normal. That is why I showed on Projection 6 the elastic energy of the support matrix. I would like to stress

at this time that we do not know enough about our magnets to decide which mechanism is the one that causes quenching, and it is this point that needs to be elucidated by much more research into their behavior.

I will now show some information that was accumulated while developing our magnet, and this evidence will show that, indeed, there were motions of the conductor in the magnet, and these were sometimes rather large.

First look at the change in diameter of a magnet as it is magnetized. Projection 7 shows the radial distortion along the diameter perpendicular to the field as a function of magnet current. This change in diameter is proportional to the square of the current and is the behavior that would be expected from elastic displacement of the support structure by Lorentz forces. These measurements were made by inventing a caliper that was read out by use of a strain gauge. Projection 8 shows the change in outer diameter, and the difference between these two changes probably represents compaction of the winding under the large forces. Projection 9 shows the histogram of this outer radial motion for the same series of magnets that we have used before. In each case, the motion is very nearly elastic, i.e., the motion for the current increasing and the current decreasing is essentially the same and is proportional to the square of the current. The value shown in Projection 9 is for 4 kA, which represents a field of about 35 kG. The amplitude of the motion that we have been discussing fits well with the calculated predictions for the elastic deflection of the collars under the magnetic forces. It should be said in passing that this type of motion, which in a synchrotron can be repeated many times, can cause fatigue failure in the collars. Tests

RADIAL DISTORTION

MEASURED BY INSIDE GAUGE

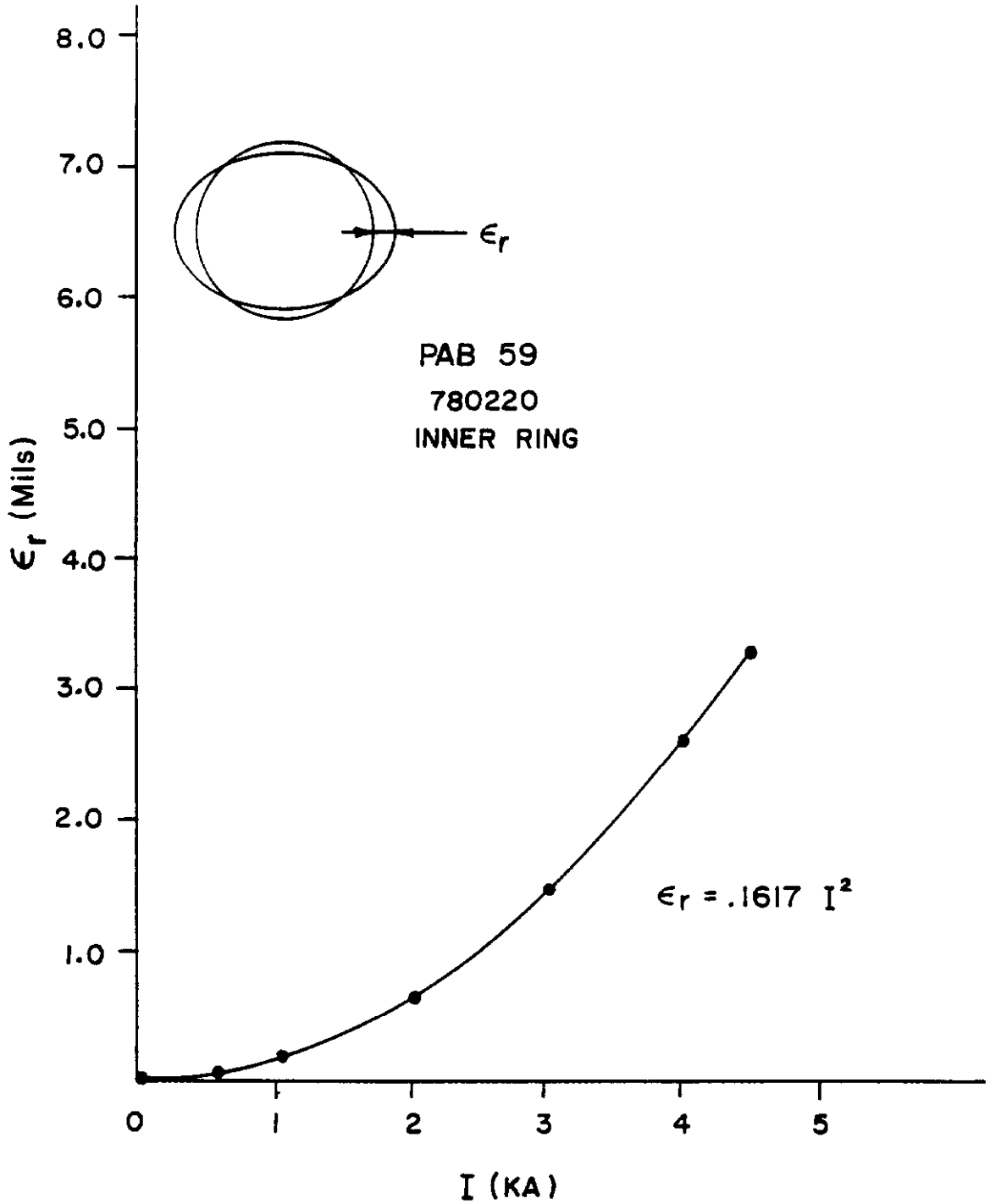

Projection 7

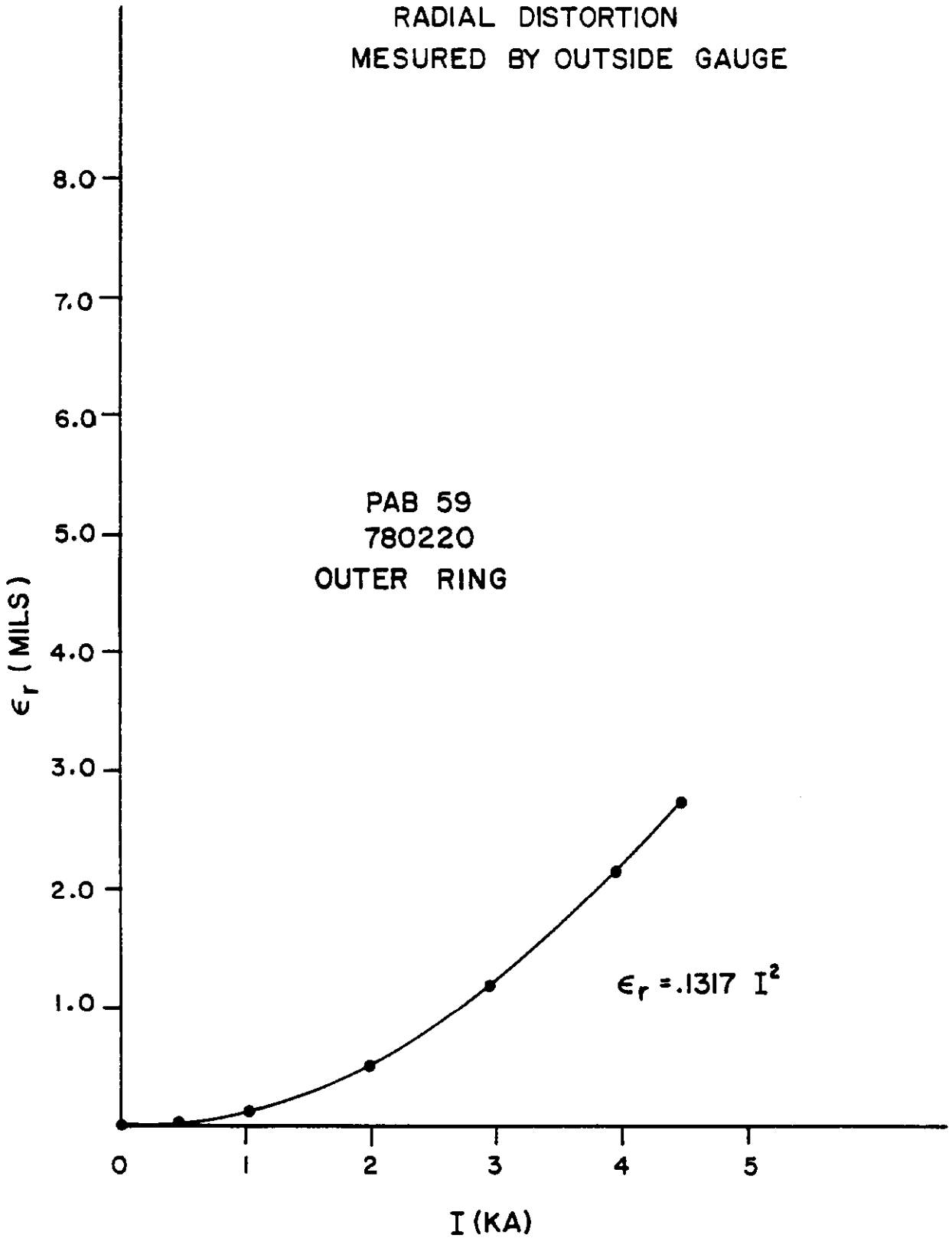

Projection 8

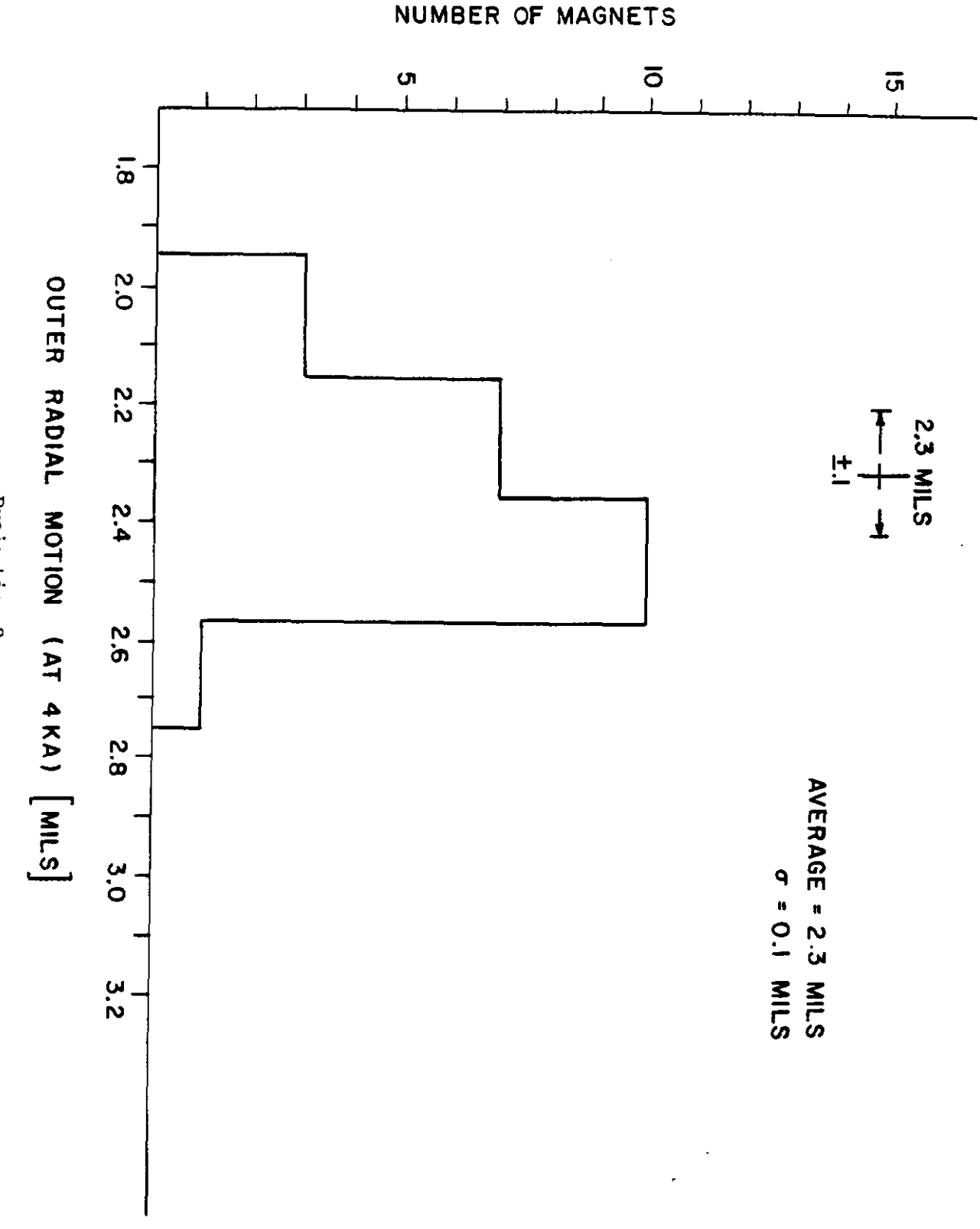

Projection 9

on the collars in the FNAL magnets originally showed that they would have failed after about 1 million cycles. The present collars show a fatigue failure time of over 100 million cycles. This difference was achieved by operating the collars at a lower stress level and relieving the points at high stress by means of rounding the sharp corners.

So far we have shown data on radial motion of the conductor. In addition to this radial motion, there is an azimuthal motion that causes compaction of the coil. This motion is predominently governed by the elastic modulus of the coil matrix itself. Since the coil matrix is not nearly as stiff as the collar, this motion can be considerably greater. Projection 10 shows the azimuthal motion of the second conductor from the end of the coil relative to the collar. Again, in this particular magnet, the motion is well fit by a parabola and is proportional to I^2. Also, there is very little hysteresis in this motion as the arrows indicate on the curve. The instrument used to make these measurements has a small correction due to the elliptical deformation of the collar, and this is shown in the dotted curve underneath the azimuthal motion and should be subtracted from the top curve. This azimuthal compaction was very difficult for us to learn how to control. In some of the early magnets, the ε shown would be more than 30 mils or about 1/2 a conductor width. Such large motion was no longer fit by a simple modulus, and the nonlinear relationship gave rise to a very complicated behavior of the deflection. Furthermore, the curve for increasing current and decreasing current could be very different, the motion showing large amounts of hysteresis.

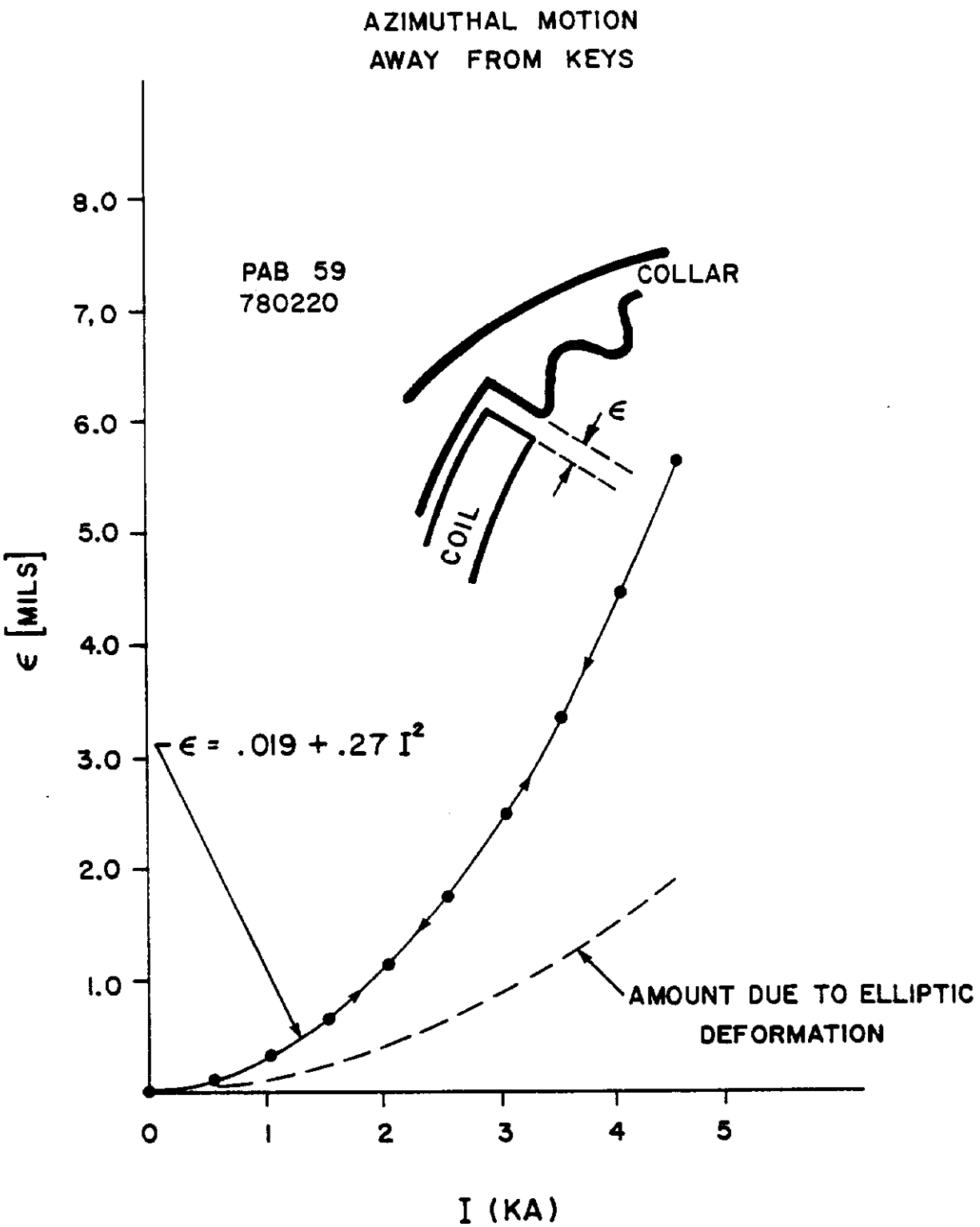

Projection 10

Projection 11 shows an attempt to display the effect of the amplitude of this motion on the training behavior of the magnet. The vertical axis displays the average amount of this motion versus the number of quenches to fully train a magnet which is shown on the horizontal scale. To make the meaning of the points more clear, I would like to explain that for instance the first point plotted at one quench consisted of averaging ε_θ for 14 magnets which were fully trained in one quench. The size of the error bars shown are the deviation of this average value in the set of 14 magnets. As long as this motion is no more than about 5 mils, it is elastic and is well fit by a parabolic motion. When it becomes greater than 5 mils, in general it means that the clamping mechanism is failing, and the collar is no longer restraining the wire. Thus, the points at 15 quenches showing motions of 20-25 mils represent unclamped conductors. This curve would seem to indicate that as long as the conductor is moving elastically, the size of the motion is not closely related to the number of quenches required to train the magnet, but that once the conductor is no longer clamped, the training is seriously affected.

I would next like to show some data that indicates that a fully trained magnet really does quench at the expected point in the winding. Projection 12 shows a view of one of the coils, both as a projection looking at the top and a cross section looking at the end. Point No. 2 is the high field when the magnet is inserted inside of an iron yoke. The peak B at Point 2 is about 10 percent higher than the B at the center of the magnet. On the other hand, when the magnet is tested without an iron yoke, the high field point moves

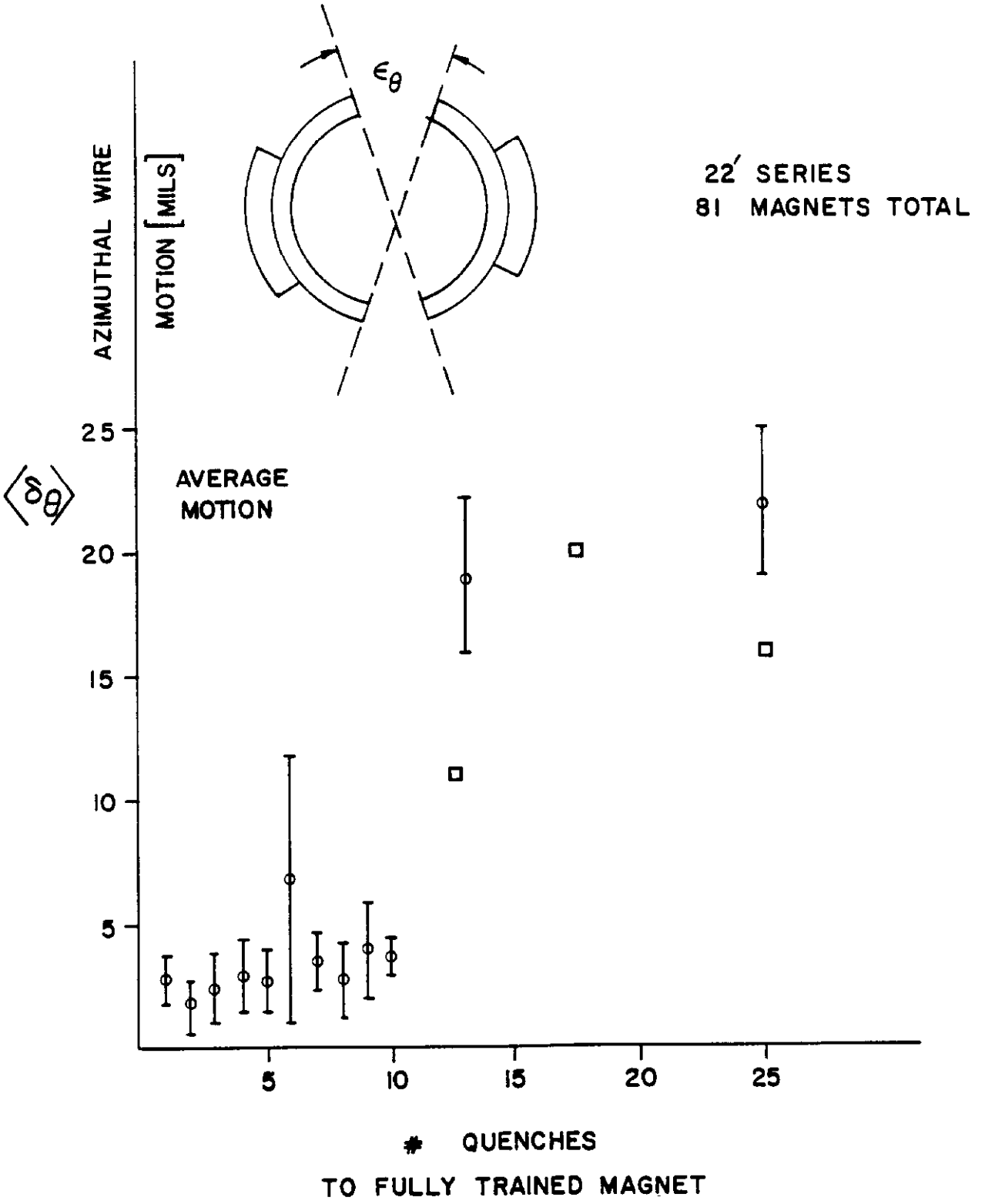

Projection 11

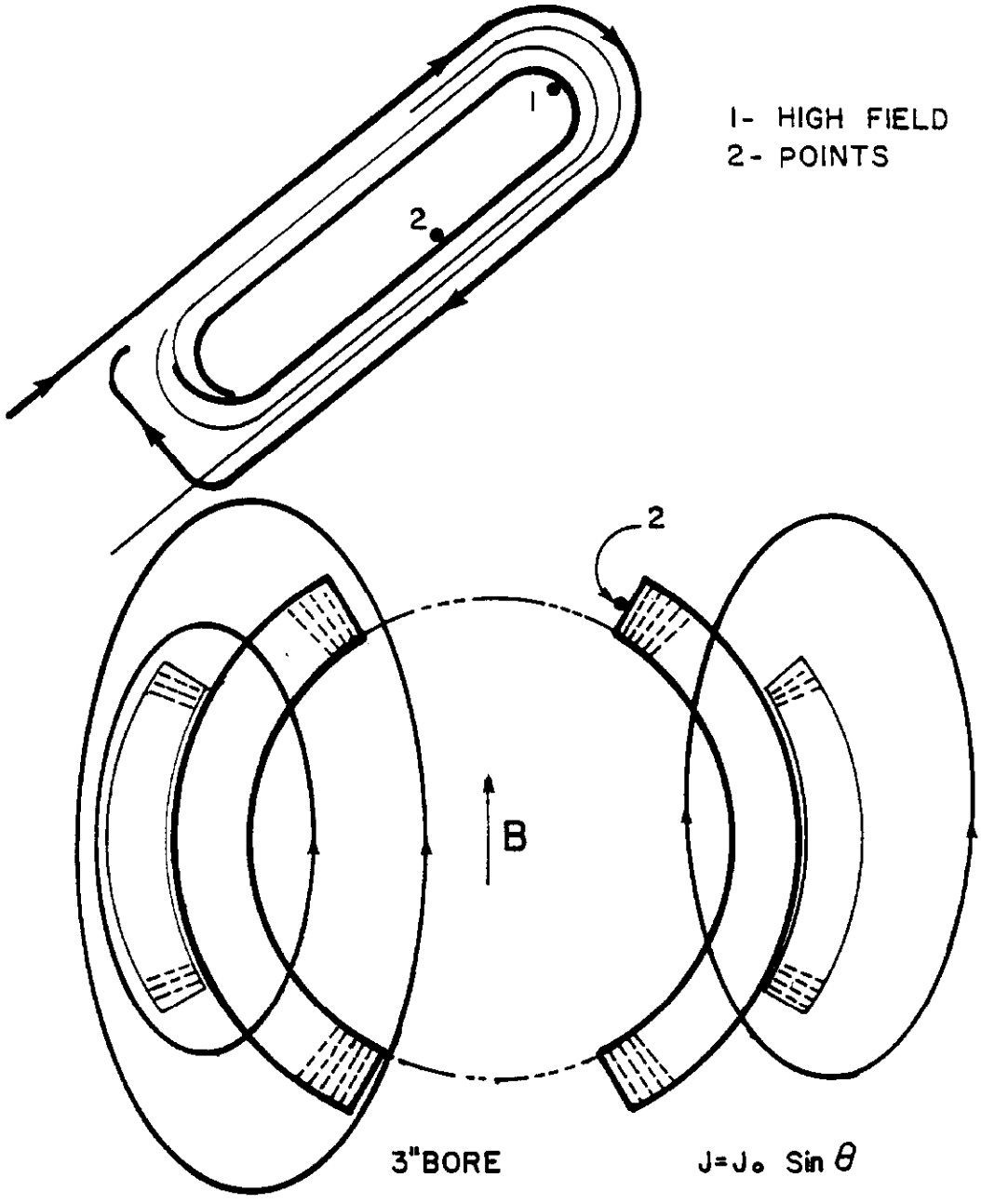

Projection 12

to the inside turn at the end of the inner shell of the magnet, shown as Point 1. The field at this point is about 20-22 percent higher than the field on the axis of the coil. Projection 13 shows the relevant data for a 22 ft. magnet tested without the iron yoke. The straight line represents the maximum field point in the coil as a function of the current. The curved line represents the wire characteristics as determined in the short sample test for the cable that was used in this magnet. The points along the magnet load line represent the individual quenches that took place as the magnet was trained. It is seen that the magnet gets to about 96 percent of its short sample limit. This type of behavior is typical for the magnets that we have been talking about. I would now like to demonstrate that for one of the 1 ft. model magnets the quench did take place in the fully trained magnet at the expected high field point. In order to understand these measurements, we will have to investigate the subject of quench waves.

Projection 14 shows what happens to a conductor when a section of it goes normal. At the bottom of this projection we see a diagram of the temperature along the axis of the wire when one section of it has gone normal and is carrying a high current. The I^2r loss in this part of the wire when it is carrying 5,000 amps is about 25 watts per centimeter of length. This heat generation is so high that the helium in contact with the wire is not capable of keeping it in the superconducting state. Consequently, more of the wire is driven into the normal condition, and a quench wave propagates out from this region with a velocity v_q. The characteristics of these quench waves were studied in the experiment shown schematically at the top of the projection. A hairpin about 12 in. long of 23 conductor cable was immersed

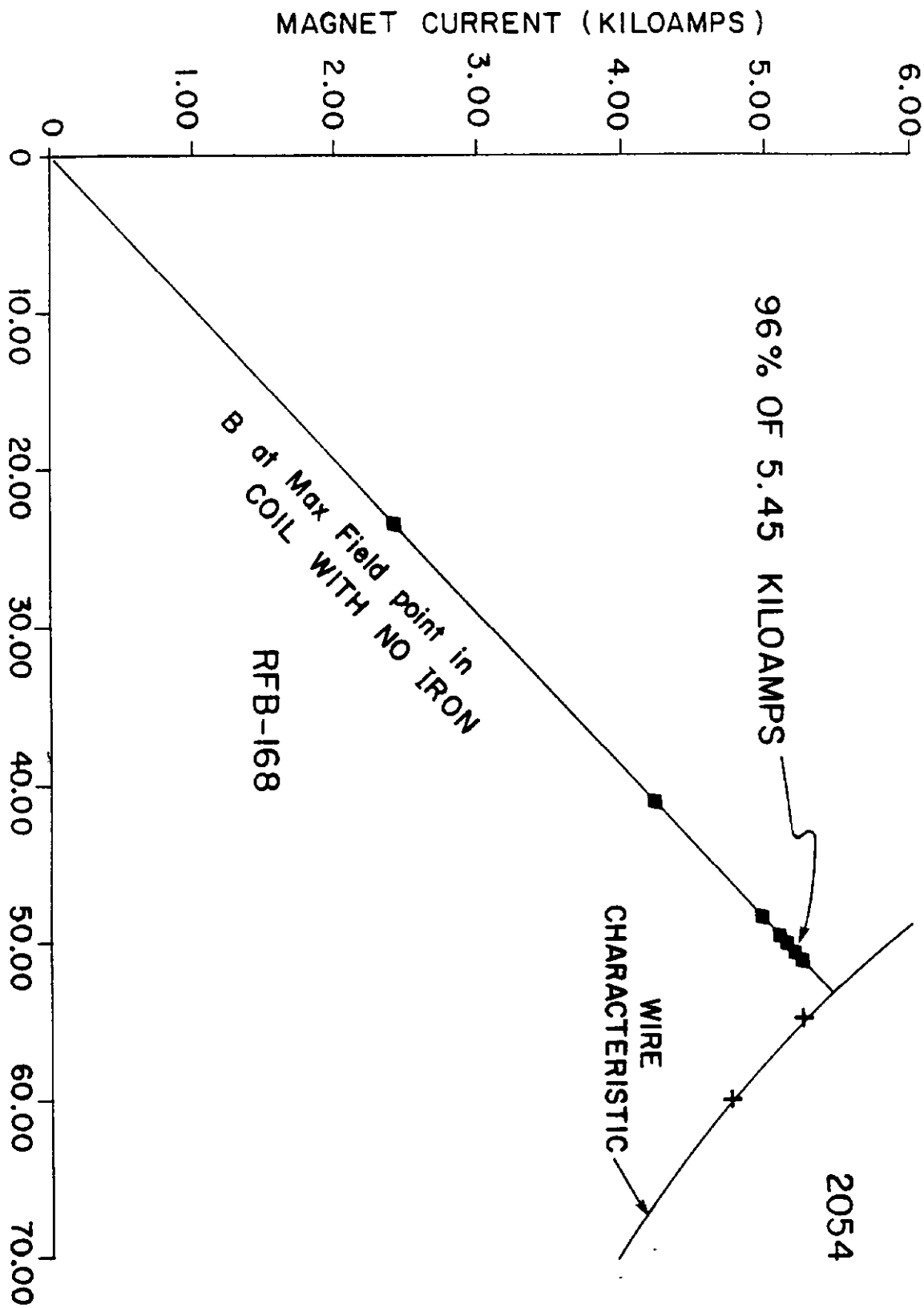

Projection 13

QUENCH WAVE MEASUREMENTS

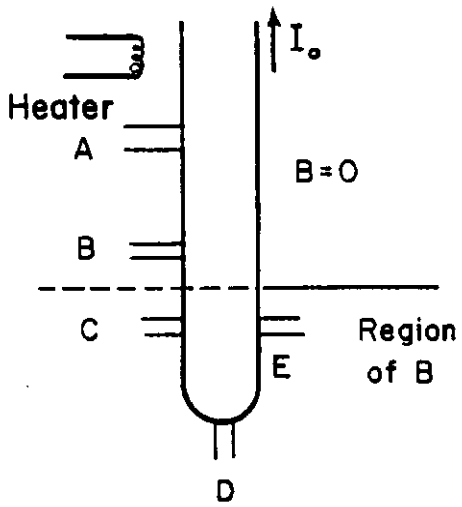

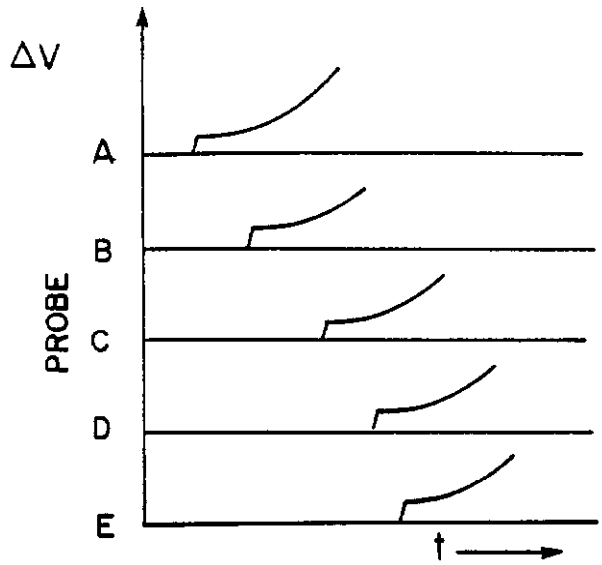

Probe response VS t

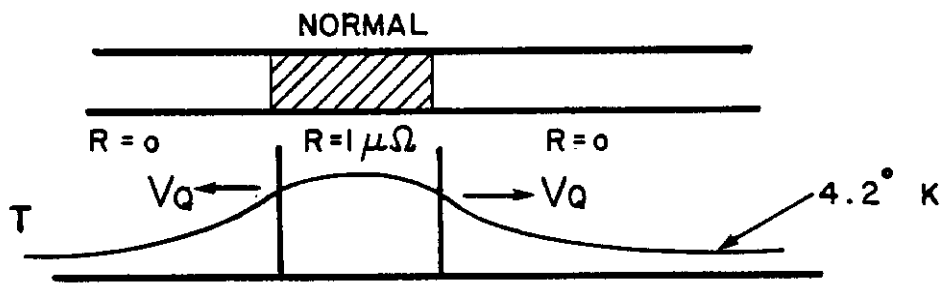

I^2 R = 25 Watts / cm of wire
at 5000 Amps

Projection 14

in liquid helium. It had little dipole contacts labeled A, B, C, D, and E located along its length. The bottom part of the hairpin was embedded in a high field region, and the value of B in this region could be controlled separately. The hairpin carried a certain current I_o, and a quench was initiated in the conductor by means of a heater that could be pulsed. As the quench wave propagated down the wire, it would become normal, and the dipole probes connected to a chart recorder showed the voltage drop across a centimeter length of the conductor as a function of time. This is diagrammed at the top right of the projection. By measuring the time of the appearance of the wave at various probes and knowing the distance between them, one could calculate the velocity of the quench wave and study this dependence upon B and I_o.

Projection 15 shows the results of some of these measurements. The bare conductor is shown as well as the conductor that was insulated with mylar in a fashion similar to the conductor used in the magnets. It is seen that quench waves do not propagate below a current of about 1,000 amps and that their velocity, once they start, is several meters per second and is roughly linearly dependent upon the current being carried in the conductor. We also compare in this projection a single strand where we have multiplied by 23 the current in order to put it on the same horizontal scale. It is seen that the cooling of a single bare strand is somewhat better than that of the cable as a whole. Projection 16 shows the behavior of the quench velocity in a single strand as a function of the current through it and as a function of the magnetic field in which the conductor is immersed.

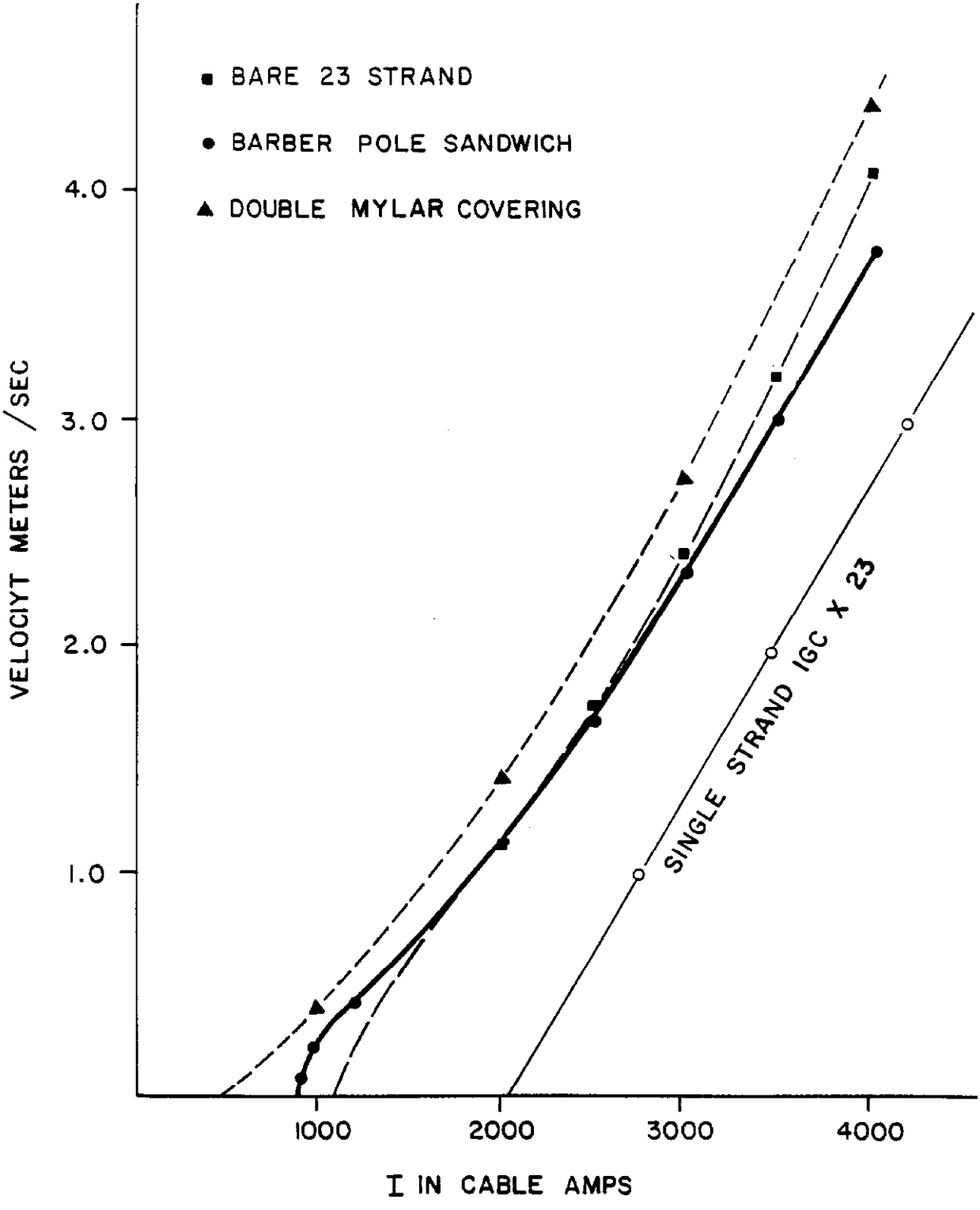

Projection 15

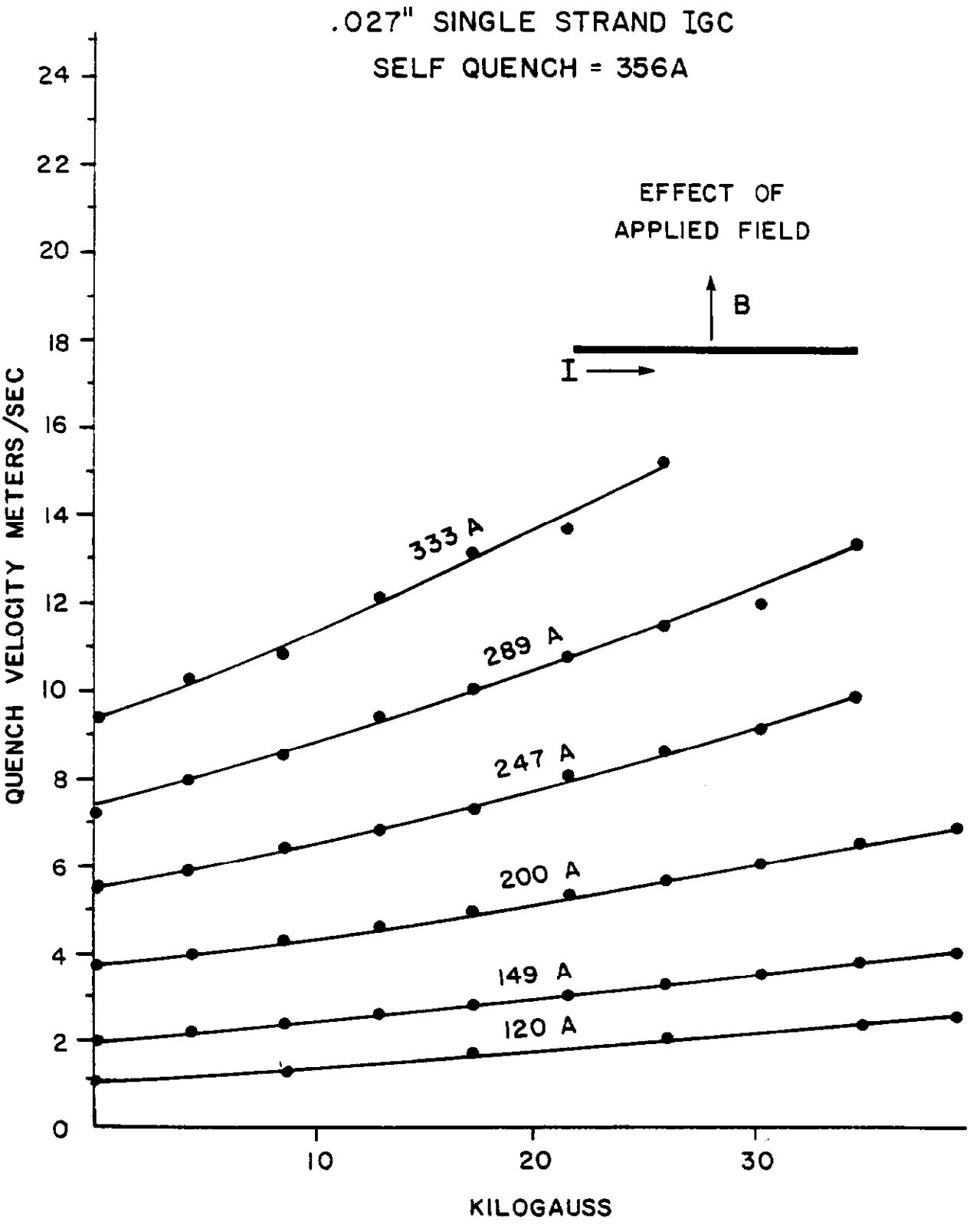

Projection 16

Figure 17 shows the results of using quench waves to locate the position of a quench in a fully trained 1 ft. magnet. Multiple sets of dipole probes were located along the conductor on each side of the points labeled X and Y. These probes were connected to a chart recorder. The magnet was then pulsed slowly until it reached its high field limit and quenched. The high field point is represented by a cross about 1/2 way between the points X and Y. There were enough probes located on the winding so that one could determine both the velocity of the quench wave and the point where it started. The histogram at the bottom of the drawing shows the location of the point where the quench started. It is seen that within a few millimeters the coil was quenching at its high field point. This experiment demonstrates that a fully trained magnet upon reaching its short sample limit, quenches at the point predicted by theory.

There are other ways of demonstrating that a magnet is operating at its short sample limit. The data in Projection 18 was obtained by Bill Sampson at Brookhaven. This was a magnet that exhibited a fair amount of training. For these measurements, the temperature was varied. Since one knows the behavior of the short sample limit of the conductor as a function of temperature and one knows where the high field point is located in the magnet, one can make a predicted curve of current versus temperature. The predicted curve is shown as a solid line and the measured points as circles slightly below this line. The feature that is interesting to observe is that at a temperature of about 5.5°, the quench current no longer increases; it levels off. It was concluded that this magnet was no longer quenching at its short

QUENCH ORIGINS

E1-12 no Iron

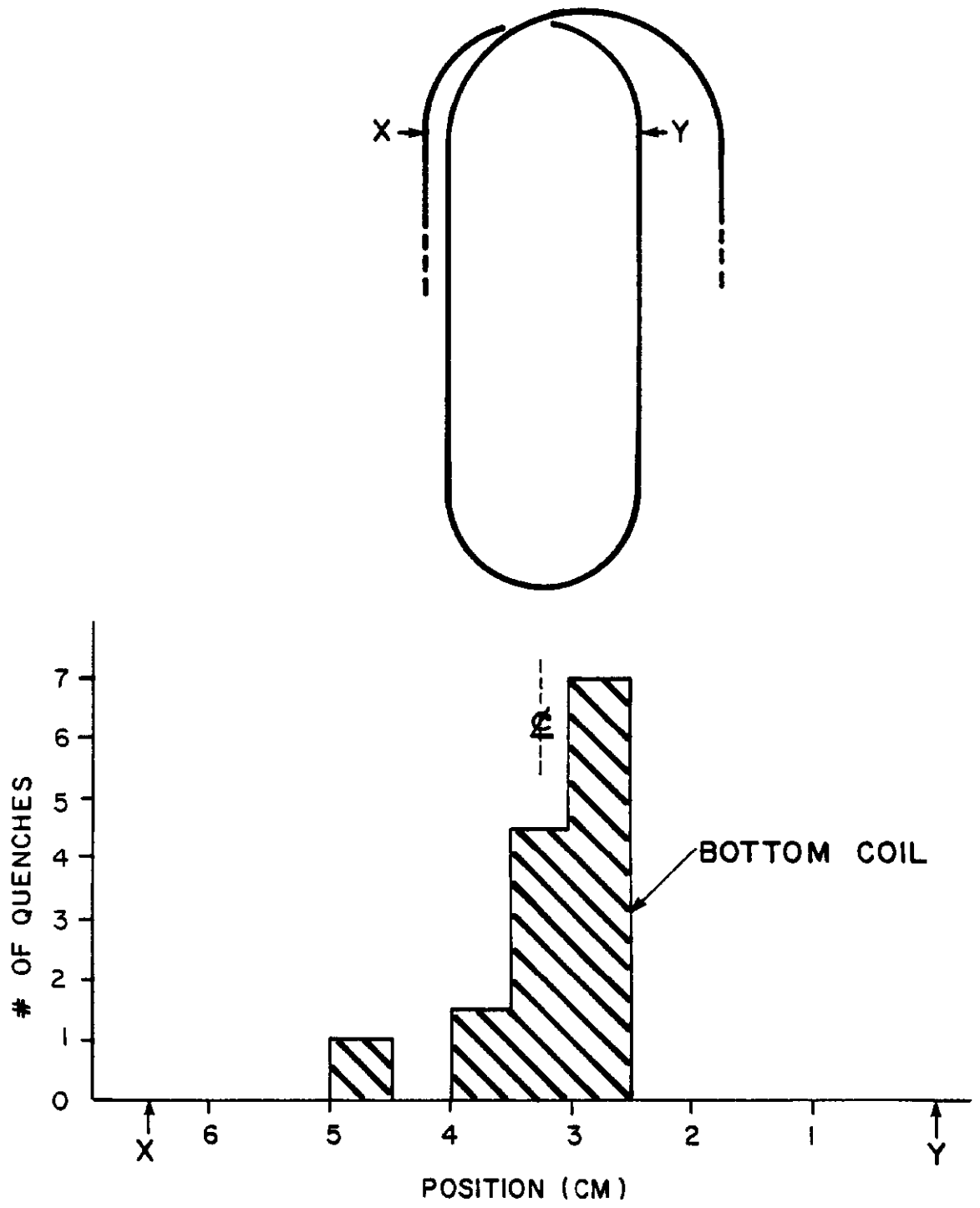

Projection 17

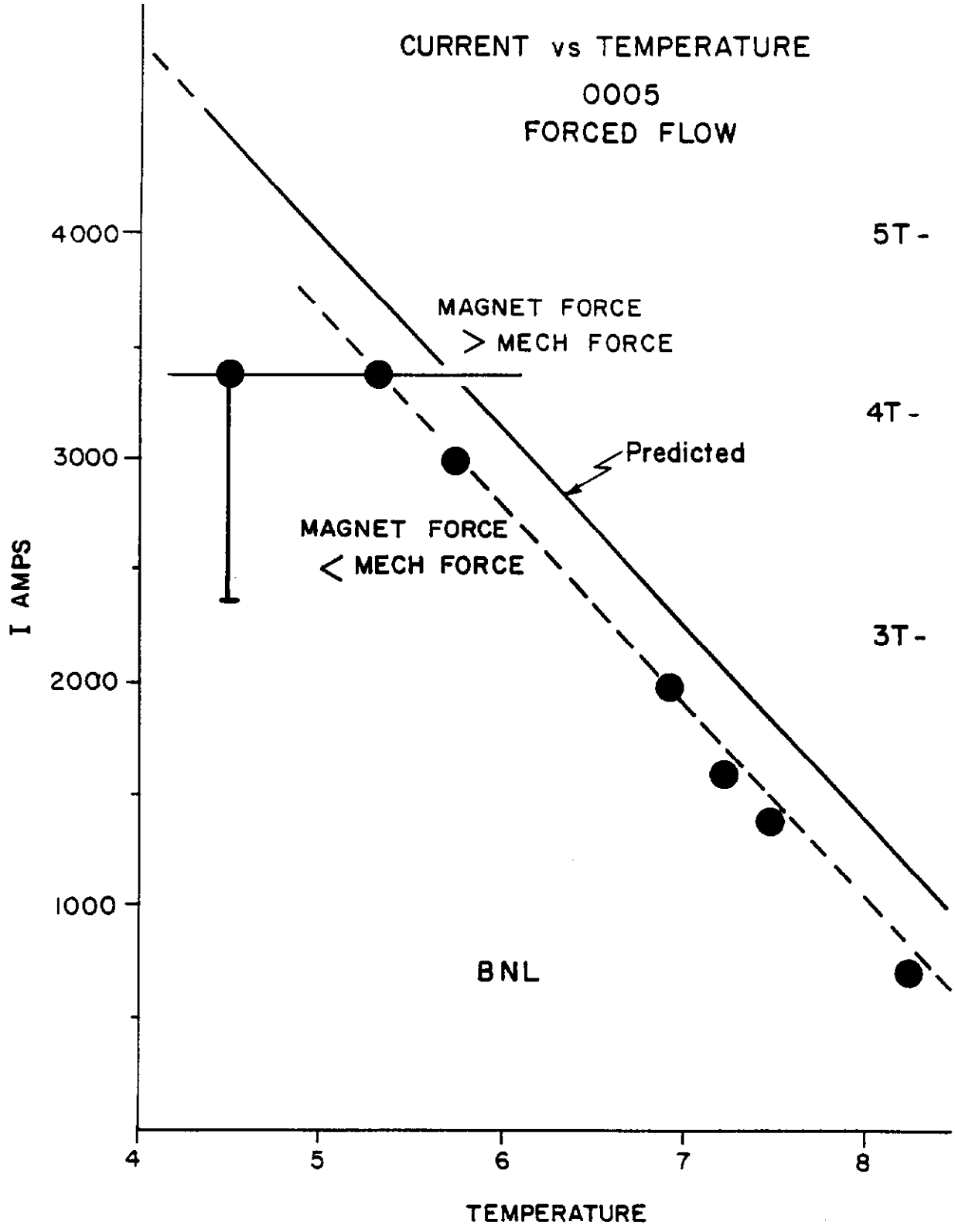

Projection 18

sample limit due to the fact that the magnetic forces were greater than the mechanical forces of constraint and that the conductor was moving. It is thought that the conductor motion was causing premature quenching of the magnet.

Figure 19 shows some data obtained at LBL on some ESCAR type magnets. This curve plots the variation in the quench field as a function of the ramp rate. We will discuss this type of curve in more detail in a few minutes, but the ramp rate induces additional heating into the magnet through eddy current effects and causes the maximum B observed to decrease as a function of $\dot{B}$. The data obtained in this case show the result of increased clamping of the conductors. The highest curve for the tightest clamping was at the short sample limit of the wire for the magnet. Again, we have a situation where motion of the conductor seems to cause premature quenching of the magnet.

I would like to summarize this situation briefly at this point. I've shown data on a large series of magnets that did not have serious training and went close to the short sample limit. These magnets all displayed elastic motion with little hysteresis. Once this motion becomes large due to lack of clamping, and there is resultant frictional motion of the conductor, then magnets may take many quenches to train and sometimes may not even reach the short sample limit. This is indicated in the two examples shown of a magnet from LBL and one from Brookhaven. In addition, at Fermilab we have observed many times that the magnetic field shape changes during training as well as the mechanical dimensions of the magnet. Apparently, the process of training results in permanent shifts in the placement of the conductor. Once the conductor is in some type of stable location, the training effects cease, and the magnet tends to go to its short sample limit.

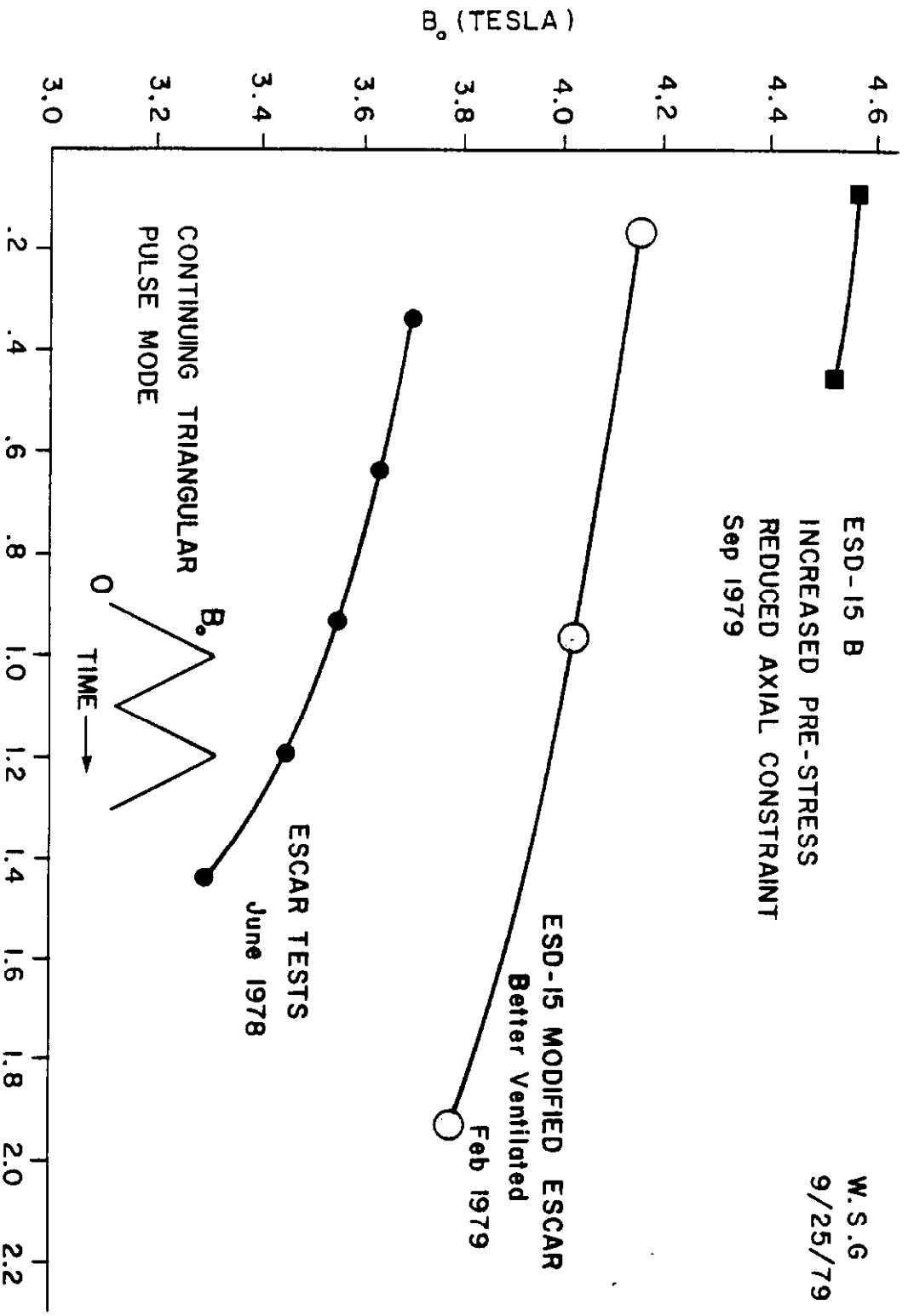

Projection 19

Next let's consider the subject of strain in the matrix and how it effects the quenching and training of a magnet. It has been known for some time that epoxy in intimate contact with the conductor of a superconducting magnet will generate a situation in which an excessive amount of training is displayed. Projection 20 shows an extreme case in a magnet constructed at FNAL. The conductor for this magnet was the same as it was in the series of magnets that showed rather little training. However, it was spray coated with a very thin film of epoxy before the magnet was constructed in an attempt to solve a turn-to-turn short problem that we had at that time. This was a 1 ft. magnet, and magnets in this series could generally be expected to train in no more than 10 quenches. It is seen that this magnet trained slowly and that it never reached the short sample limit. The dips in the curve are caused by ramp rate tests and should be disregarded in this discussion. This experiment was repeated on several identical magnets with similar results.

Figure 21 shows an attempt to understand whether or not the cracks in the support matrix of a 22 ft. long magnet were actually associated with its training. The horizontal axis is the current through the magnet on any given cycle. The vertical along each curve shows the noise pulses as detected by a microphone connected to the magnet structure. For instance, the first curve shows noise pulses up to a current of about 2,500 amps at which point the magnet quenched. The next cycle shows that the noise pulses were absent until the current of the first training cycle was exceeded, at which point noise again appeared. This could be interpreted as the support matrix cracking and failing as higher and higher force levels in the magnet are reached.

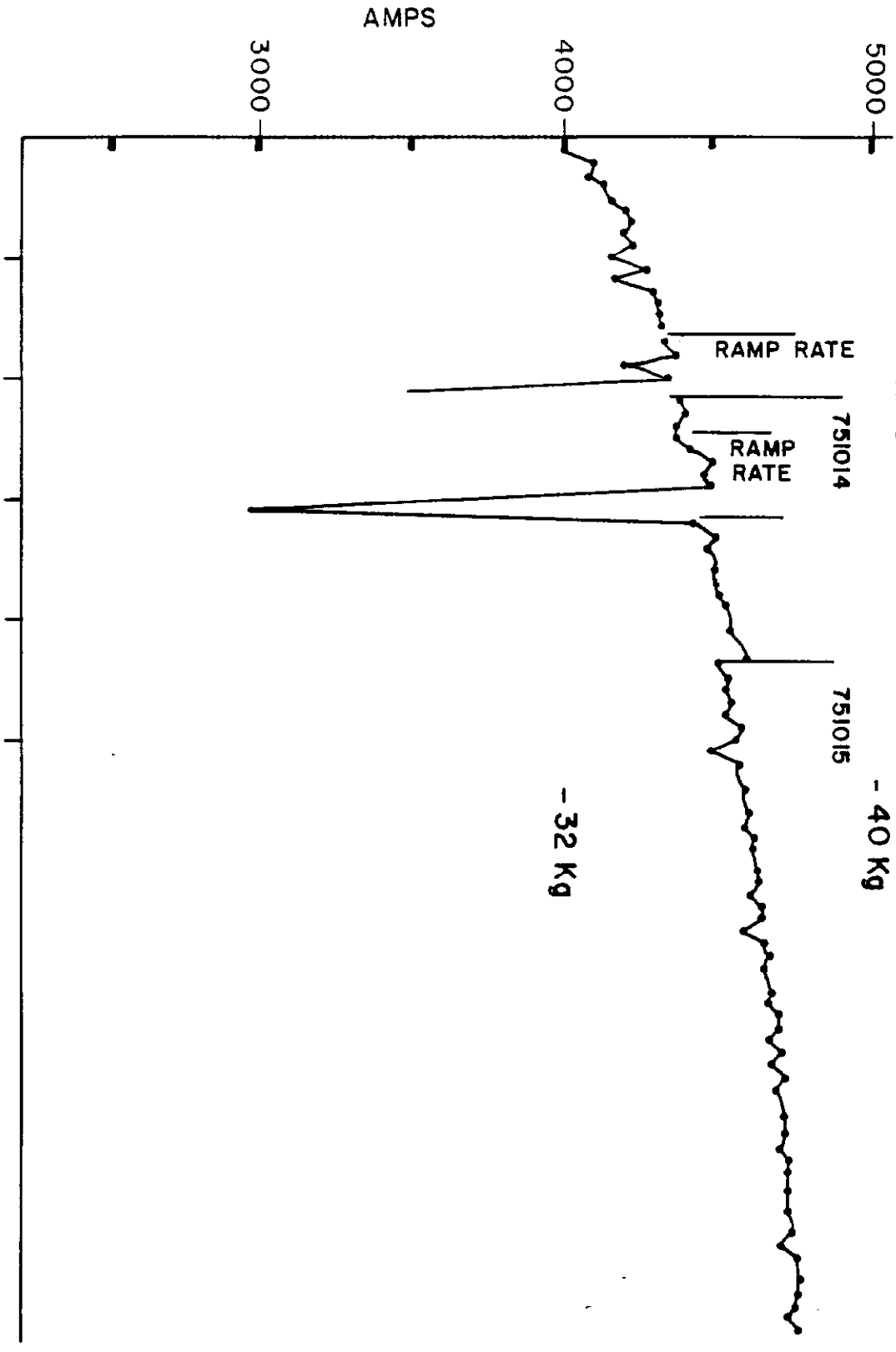

Projection 20

HELLUM MICROPHONE
NOISE EVENTS IN E1-6

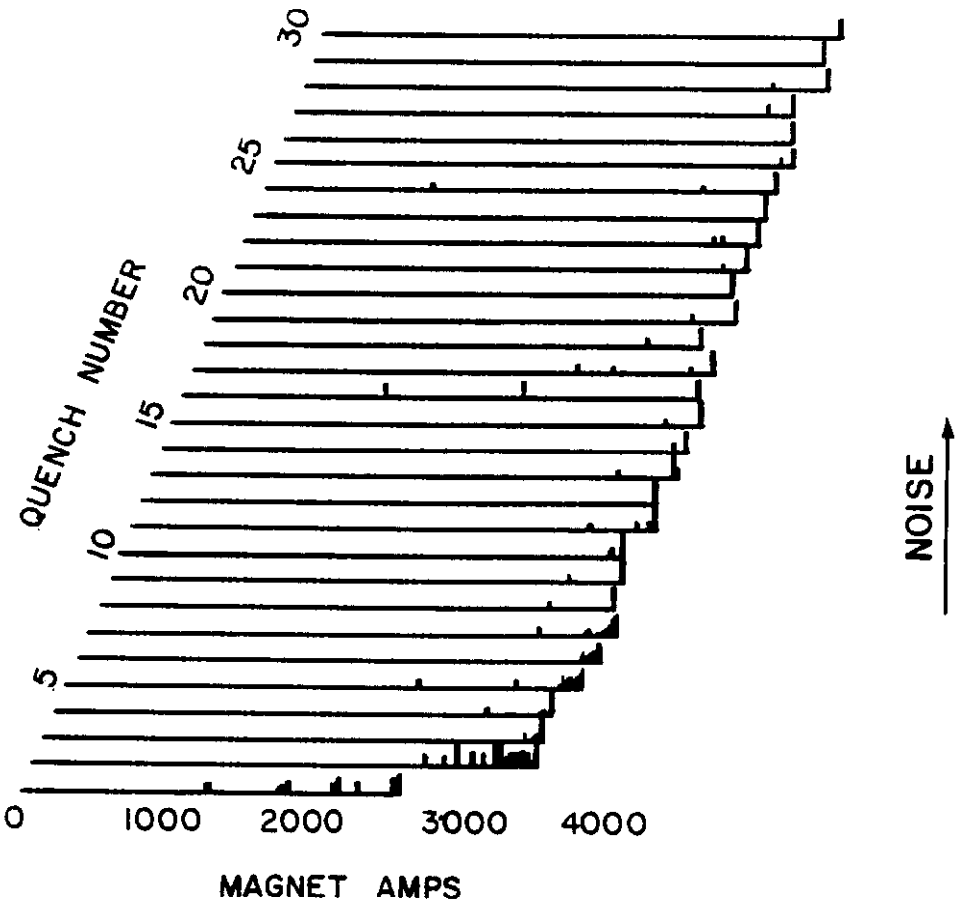

Projection 21

Finally, on the 30th quench, the magnet was fully trained, and it is seen that the noise pulses have completely disappeared. This type of experiment is suggestive that cracks in the support matrix are contributing to the training process but as a definitive experiment, it leaves something to be desired.

There is yet another parameter that can influence the quenching of a coil. This situation arises when a correction coil is placed inside of a dipole or quadrupole magnet or when several correction coils are wound together on one mandril. A coil then finds itself immersed in the field of a second coil. Thus, the maximum B of the coil is not determined by the current through the coil itself but by the current through the coil plus the applied external field. Projection 22 shows the results of measurements made at Fermilab on a dipole correction coil intended to be used inside of one of the quadrupoles. These elements are used for trimming the orbit and compensating for errors in the main bending dipoles. The curve across the top of the figure represents a short sample limit of the wire. The vertical axis is the current through the coil, and the horizontal axis is the magnetic field at the high field point. The various curves that have shifted parallel to each other represents the effect of an applied external field. Projection 23 shows the training curve of this correction coil. It was first started off with zero applied external field and trained up to about 140 amps. An external field was then applied at Quench No. 20, and it was necessary to again train the magnet. These results will be presented in more detail in the correction coil session. I want to mention them here because it represents a difficult training problem that must be solved whenever the external field in which a coil is immersed is changed. This action may require retraining the coil.

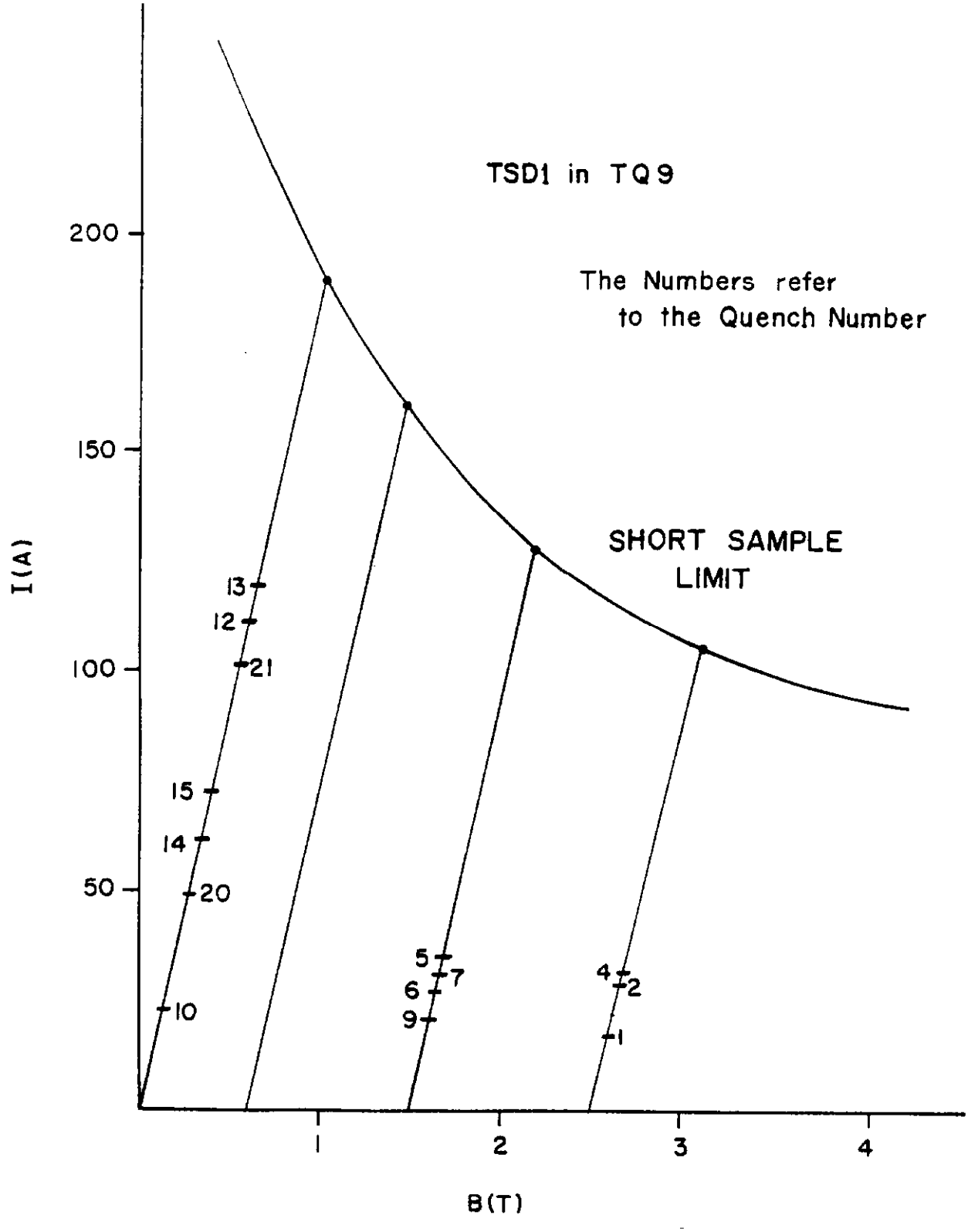

Projection 22

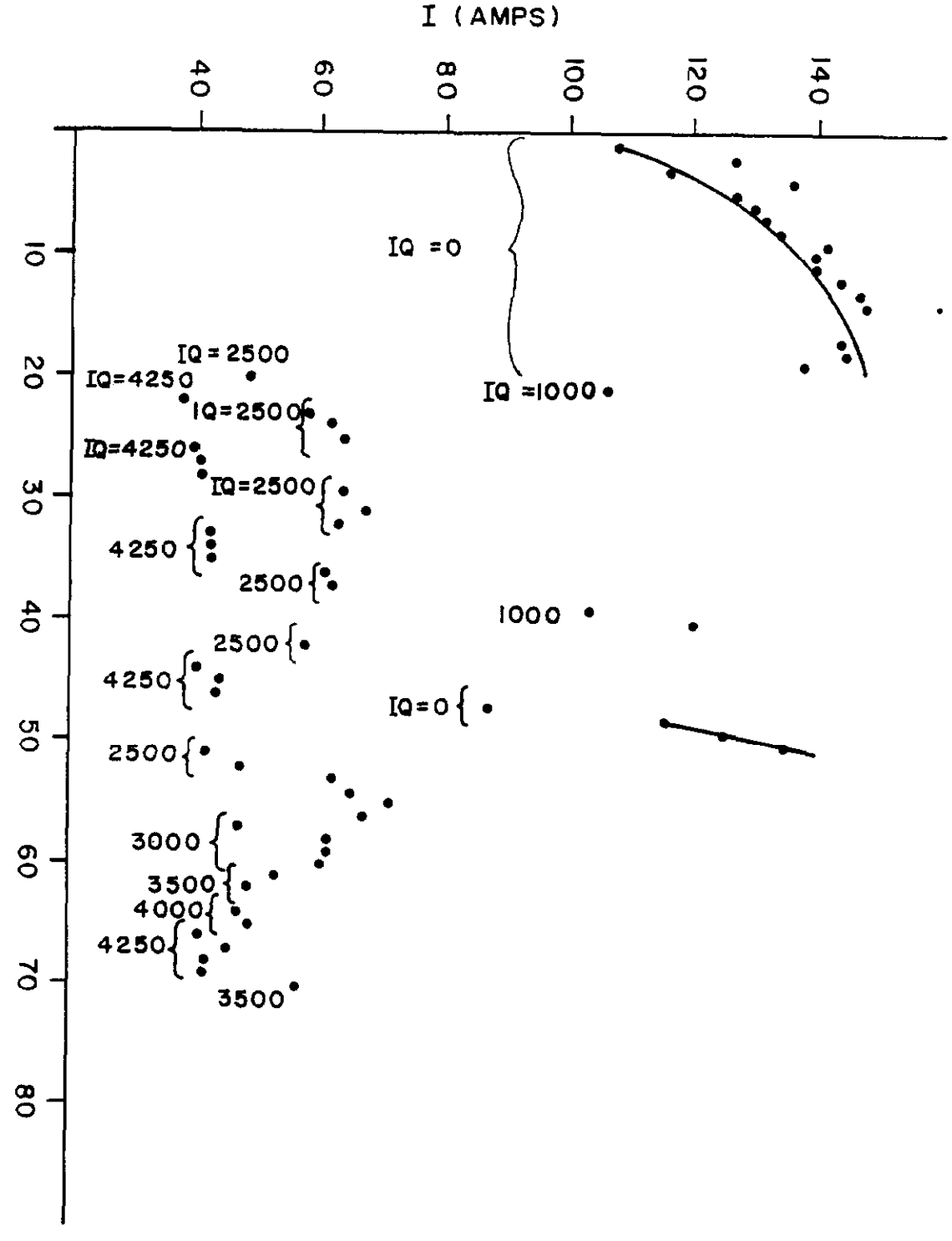

CORRECTION COIL TRAINING

Projection 23

The problem can be enhanced if the relative directions of the fields can reverse because of the desired correction. It would be very useful if we could learn how to construct a coil for this type of application with a minimum amount of training. The fact that the training recommences when the forces are redistributed would suggest that in each case the wire is finding a new equilibrium position.

So far we have been discussing quenches observed when the magnetic field is changing very slowly. However, a synchrotron involves a rapidly pulsing magnetic field. The pulsing of the field can induce eddy currents in the coil and cause heating. This heating can cause the coil to quench at a lower current than is observed when the $\dot{I}$ is very slow. We look briefly at the theory of this process.

Projection 24 shows why a pulsing magnet heats up. First of all, there are persistent currents that flow in the volume of the superconductor itself. This generates a magnetization M per unit volume, and this magnetization is an open loop. The first curve shows such a loop of magnetization as a function of B, and it is observed that the energy loss per cycle is proportional B_{max}.

Eddy currents can also exist in the matrix. In this case, we find that the EMF is proportional $\dot{B}$ and as the bottom of the figure shows, the Joules per cycle in this case are proportional to B_{max} times $\dot{B}$. Projection 25 shows the behavior of the Joules per cycle as a function of B_{max} holding $\dot{B}$ fix and as a function of $\dot{B}$ hold B_{max} fixed. By measuring these curves individually,

$\dot{B}$ INDUCED QUENCHES

pulsing a magnet heats it !

I-

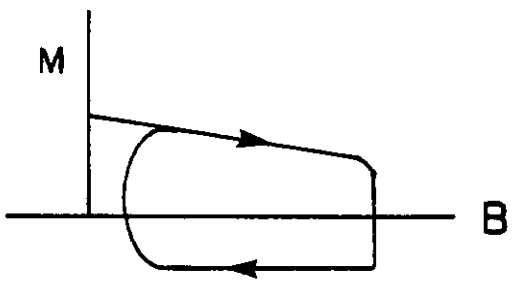

$$J/\text{Cycle} \sim B_{max}$$

II- Eddy currents in matrix

$$\text{Emf} \sim \dot{B}$$

$$\text{Power} \sim \frac{(\xi mf)^2}{R}$$

$$\sim \frac{\dot{B}^2}{R}$$

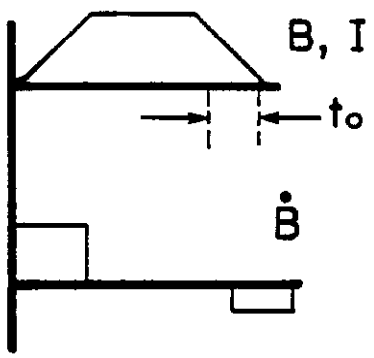

$$J/\text{Cycle} = Pt = \frac{\alpha \dot{B} \dot{B} t_o}{R} \qquad \frac{B_{MAX} \dot{B}}{R}$$

TOTAL

$$J/\text{cycle} \sim \alpha B_{MAX} + b B_{MAX} \dot{B}$$

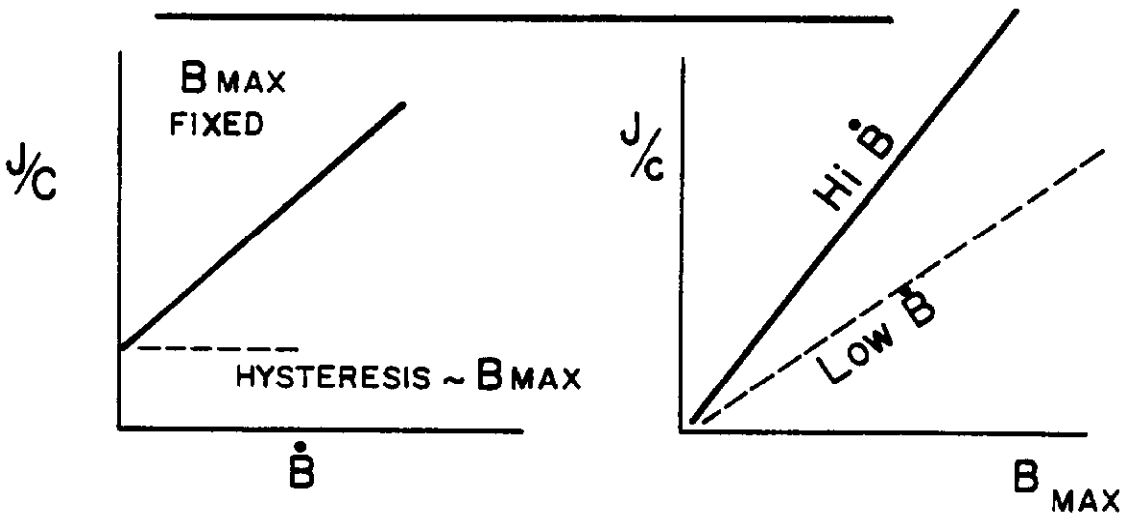

Projection 25

we can separate out the hysteresis loss from the eddy current losses. Projection 26 shows the actual quench dependence of two different magnets as a function of $\dot{B}$. The 22 ft. magnet shows a much bigger effect of pulsing than the 1 ft. magnet did. This effect is not understood, but these curves amply demonstrate the behavior of superconducting magnets under pulsed field conditions. Both of these magnets were fully trained.

Our early magnets were constructed of a cable where the 23 strands were individually covered with Stabrite, which is a silver tin alloy. The conductors were in rather intimate contact with each other, and the eddy current losses in this matrix were quite high. In fact, the losses were so high that steps had to be taken to reduce them. We investigated coating every other strand in the cable with an insulating covering. This insulation consisted of ebonol, which is a copper oxide coating applied to the outer copper jacket of the strand. Projection 27 shows a comparison between two 22 ft. magnets, one of which was constructed with Stabrite coated cable, and the second used a cable which we call zebra conductor where every alternate strand is coated with ebonol. It is seen that in each case at fixed $\dot{B}$, the losses are proportional to B_{max}, and that zebra type conductor has considerably smaller losses. Projection 28 shows the behavior of these losses at fixed B at varying $\dot{B}$. The intercept at zero $\dot{B}$ represents the hysteresis loss in the conductor and should be the same in the two magnets. It is seen that the eddy current losses in the Stabrite are large, and that the zebra conductor virtually eliminates this source of energy loss. One might expect a considerably different dependence of the quench current on the ramp rate between these two types of magnets. However, Projection 29 shows essentially the same behavior for these

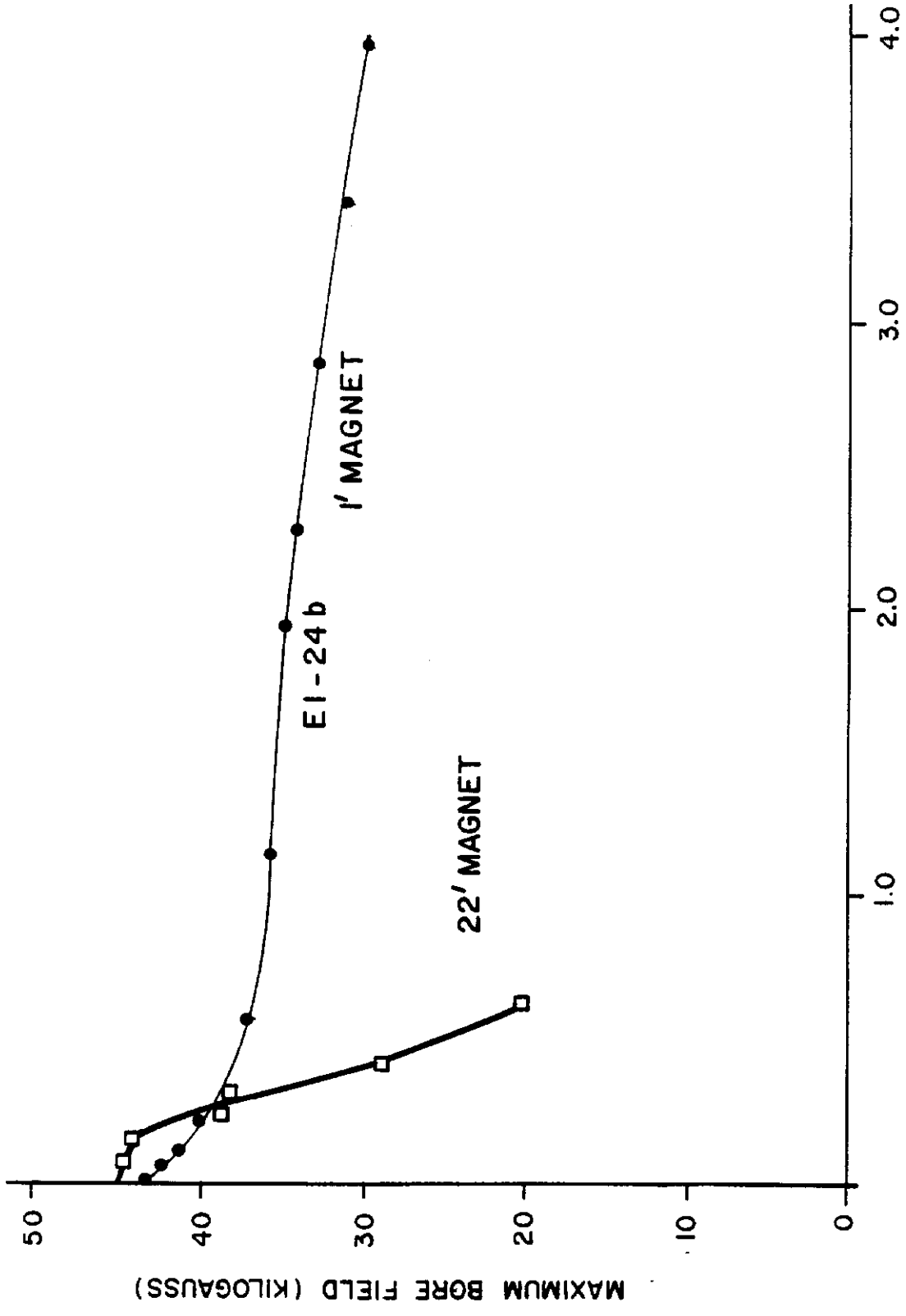

Projection 26

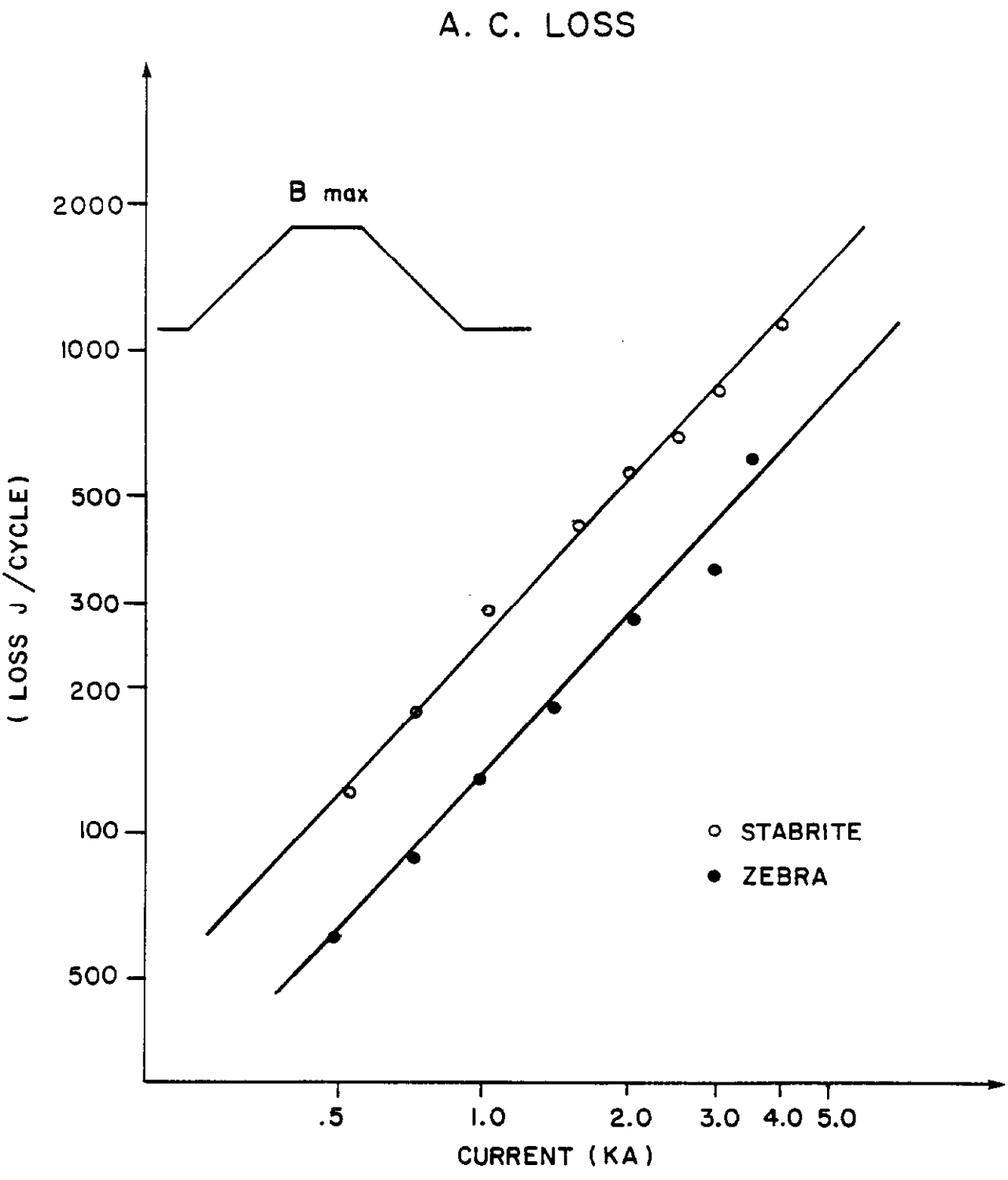

Projection 27

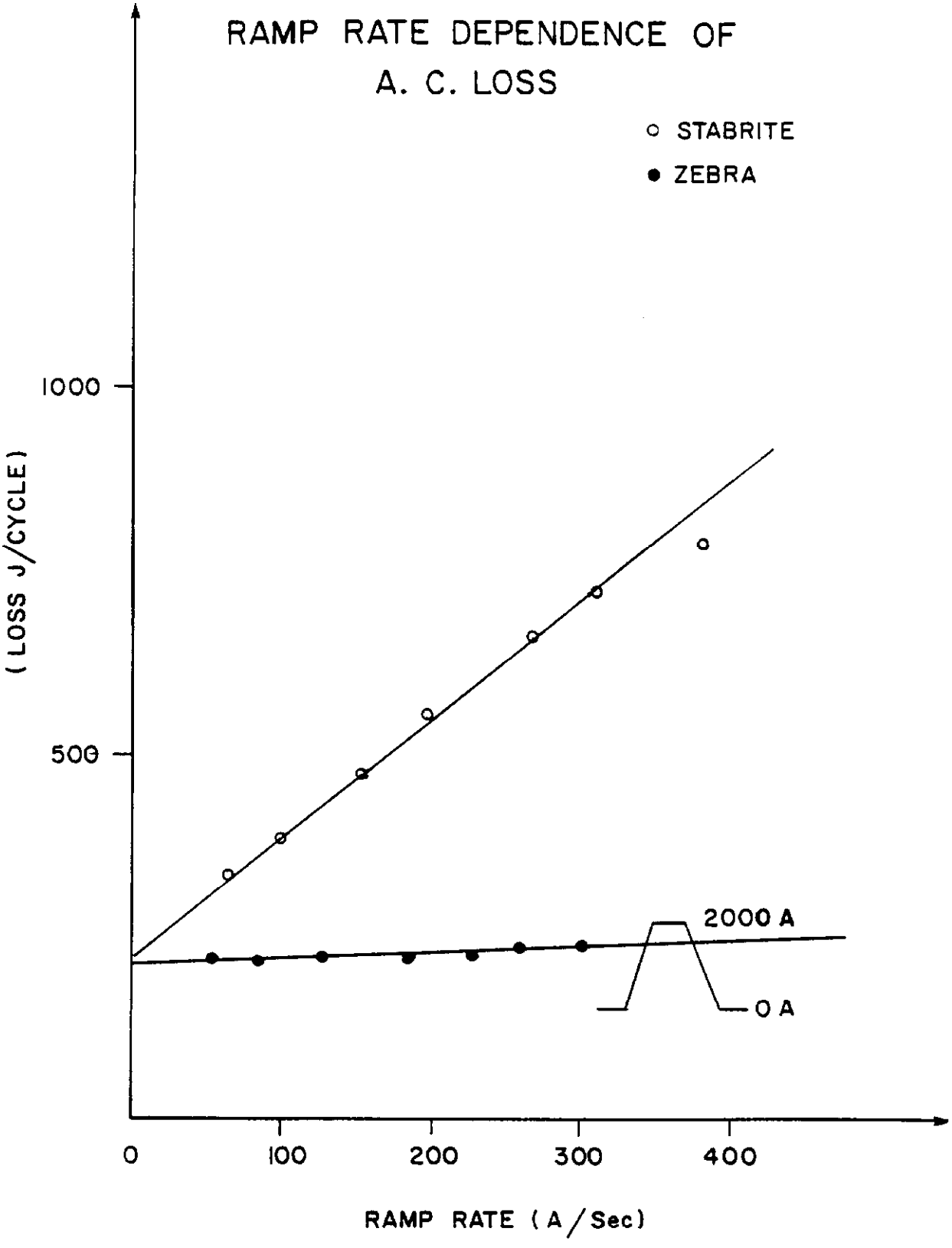

Projection 28

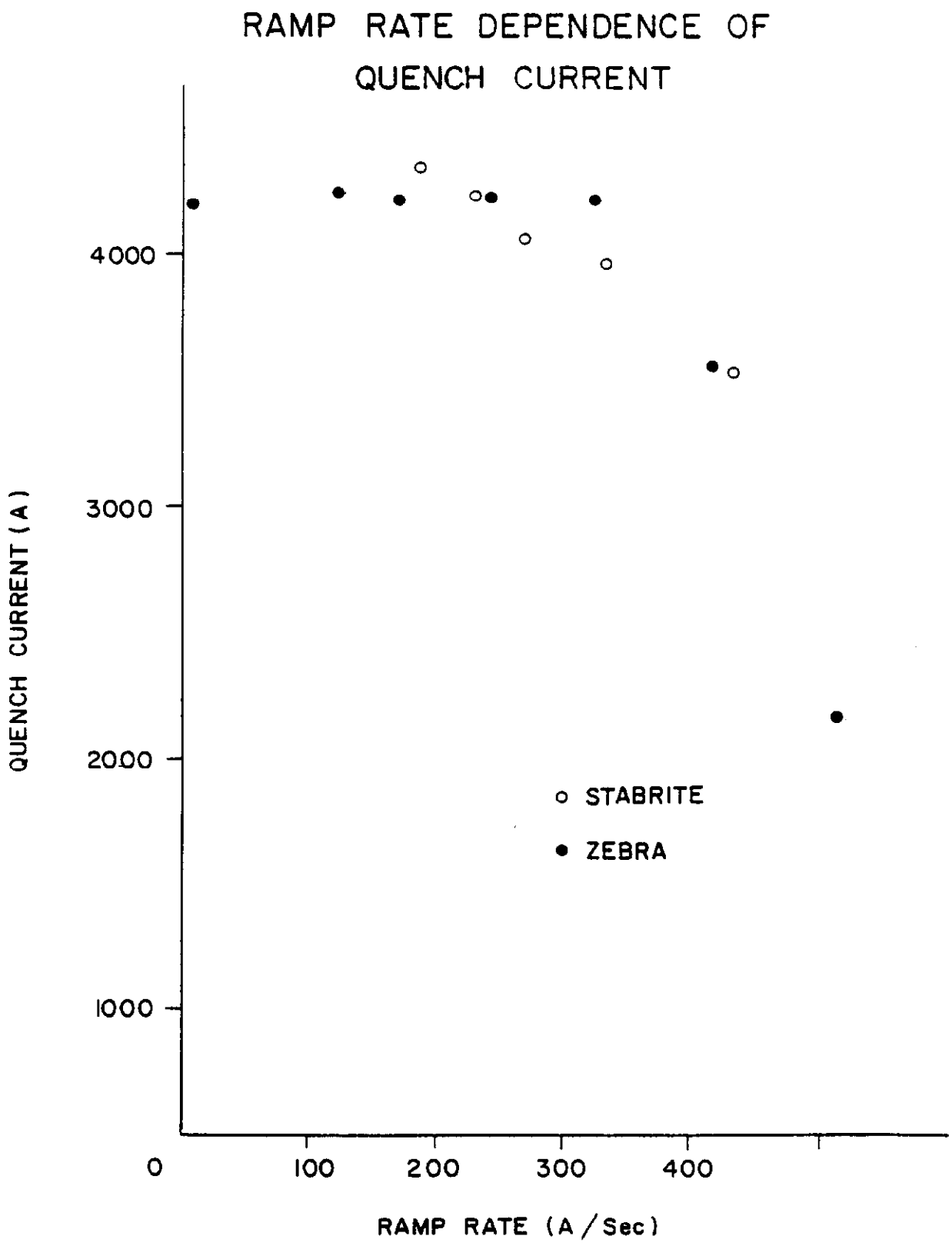

Projection 29

two cases in spite of the considerably different levels of power generated in the winding during ramping.

Questions to be Answered

From the preceding discussion, it should be clear that the behavior exhibited by superconducting magnets is not well understood. We have some emperical answers that are enabling us to produce successful magnets, but a science has not yet emerged from an art. I list some questions that must be answered by future research (Projections 30 and 31):

1. Where do quenches occur during:
   a. Training
   b. High $\dot{B}$

   It would be great to have an apparatus that would localize quenches spacially. As far as I'm aware, the measurements that I displayed on the 1 ft. magnet are the only ones that have pinpointed exactly the source of single quenches in a trained magnet. We were unable to apply this technique to a magnet during training. The quenches did not take place at the high field point.
2. What is the source of energy to start a quench?
   a. Is it wire friction?
   b. Is it cracking of the support matrix?

   I would like to make a comment on the question of the support matrix. The elastic energy stored is equal to:

$$P.E. = 1/2\ E\Delta x^2 = P^2/2E$$

where P is the pressure and is a function of B for a perfect coil and Δx is the amount of elastic strain that must be placed in the coil in order to collar it. If we had perfect coils, it is seen from the first version of this equation that the potential energy would be decreased by increasing the Youngs module of the support matrix. However, for nonperfect coils, the Δx is the more pertinent variable because the collar determines the coil size, and the displacement Δx is determined by the accuracy of the construction of the uncollared coil. If the coil is not accurately made, Δx may be much larger than that necessary to provide the forces for conductor constraint. In this case, the second version of the equation shows that the elastic energy is increased by increasing the Youngs modulus.

3. Cooling - how does it affect the quenches and the training?
   A coil that is near 4.2^{o} K has very high heat conductivity due to the copper in the cable. However, the heat capacity is proportional to T^3 and is very small. This means that the relaxation times locally observed will be exceedingly short. The dynamic transfer of heat from the wire to the cooling medium could be instrumental in changing the nature of the training. The work that has been done on using HeII at one atmosphere pressure as a cooling fluid at Saclay and at Berkeley is suggestive of interesting effects that can be observed at these lower temperatures. It could be that regardless of the material that future coils are made out of, it would be advantageous to cool them with HeII.

QUESTIONS ON TRAINING

1- EPOXY /MYLAR

NEED TO UNDERSTAND ROLE OF THE ENVIRONMENT

2- QUENCH FINDER

WHERE ARE QUENCHES DURING

a) TRAINING

b) B^{0}

3- SOURCE OF ENERGY TO START QUENCH

i) WIRE FRICTION

ii) SUPPORT MATRIX

$\delta x = P/E \qquad P.E. = \frac{P^2}{2E} = \frac{1}{2} E \delta x^2$

P. ONLY FUNCTION OF B FOR PERFECT COIL

$P \sim \delta x$ FOR ERRORS IN COIL

4- HOW DOES COOLING EFFECT QUENCHES ?

k hi, $C \sim T^3$ RELAXATION TIME SHORT

5- SUPERFLUID He ?

6- EFFECT EXTERNEL FIELDS (CORRECTION COIL)

7- WHY DOES EBONOL / STABRITE WORK

8- MORE UNDERSTANDING OF RAMP RATE EFFECT

4. What is the effect of the support matrix and what role does mylar around the cable play in the training processes for a magnet? Epoxy has been observed to be very bad in certain cases. In other cases, it seems to be good. We need to understand the effect of plastics that are in contact with the superconductor.
5. The effect of external fields upon the training of coils.
6. We need research on controlling eddy current losses within the winding. At Fermilab, we have come up with an emperical solution involving ebonol and Stabrite. Our investigation of magnets constructed of pure ebonol insulated cable indicated that the current sharing among the strands was inhibited by this much insulation, and some of the all-ebonol magnets performed very poorly, reaching perhaps only 80 percent of the short sample limit. On the other hand, some of the magnets performed very well. Why does ebonol sometimes work and sometimes not? It was observed also during this series of tests that a layer of Kapton down the center of the Rutherford cable reduced the hysteresis losses. The hysteresis losses in these measurements include not only the real hysteresis of the conductor, but also the effect of any frictional forces inside of the magnet or conductor. Perhaps Kapton was reducing these frictional losses. Additional research on this subject could lead to a significant savings in refrigeration.

7. Finally, a subject on which I have not spent any time and which is very important to understand in more detail is the question of radiation from the machine inducing quenches in the winding. Some data has been accumulated on the subject at Brookhaven and at Fermilab.

Magnet Quality and Construction Techniques

Projection 32 and 33 show the equations that determine the magnetic field in terms of the current distribution in the winding for a current shell. The vector potential has only a Z component, and inside radius r = a has terms that are proportional to r^m. The coefficients A_m are determined by the current distribution. M = 1 is the dipole field and involves the integral of the two curves shown along the right hand side of the figure. The quadrupole is equal to zero by symmetry. The sextupole can be made to vanish by stopping the winding at the 60° point. The octapole is zero by symmetry, and in the case of the Fermilab magnet, the dectapole can be made to equal zero by balancing the inside coil angle versus the outside coil angle. Projection 34 shows the quadrupole field at the top and the skew quadrupole field at the bottom. These fields will be generated by errors in the winding that cause a lack of symmetry. Projection 35 shows the results of an exact calculation by Stan Snowdon for the $\int$ Bdl through the Fermilab magnets. Out to 1 in., the field integral is constant to about one part in 10^4 for a perfectly constructed magnet. However, it is very important to recognize that the magnets that we are dealing with are different than the ones that have been used in the past. The field in each magnet is uniquely determined by the current distribution in that magnet and not by the shape of an iron conductor that

SINGLE CURRENT SHELL

$r < a$

$$A_z = \sum_m A_m \left(\frac{r}{a}\right)^m \text{Sin } m\theta$$

$r > a$

$$A_z = \sum_m A_m \left(\frac{a}{r}\right)^m \text{Sin } m\theta$$

$$A_m = \frac{2a\mu_o}{2\pi m} \int_o^{\pi} K_z(\theta) \text{ Sin } m\theta \, d\theta$$

$$B_Y(Y=0) = B_o \sum b_n X^n$$

$$B_x(Y=0) = B_o \sum \alpha_n X^n$$

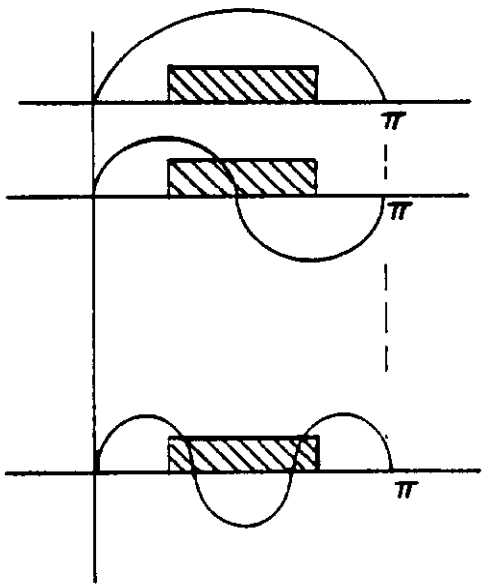

m = 1: DIPOLE

m = 2: QUAD.

=0 BY SYMMETRY

m = 3: SEXTUPOLE

= 0 IF $\theta_o = 30°$

m = 4: OCTAPOLE

= 0 BY SYMMETRY

m = 5: DECAPOLE

FIRST TERM NOT EQUAL TO ZERO

TWO CURRENT SHELLS

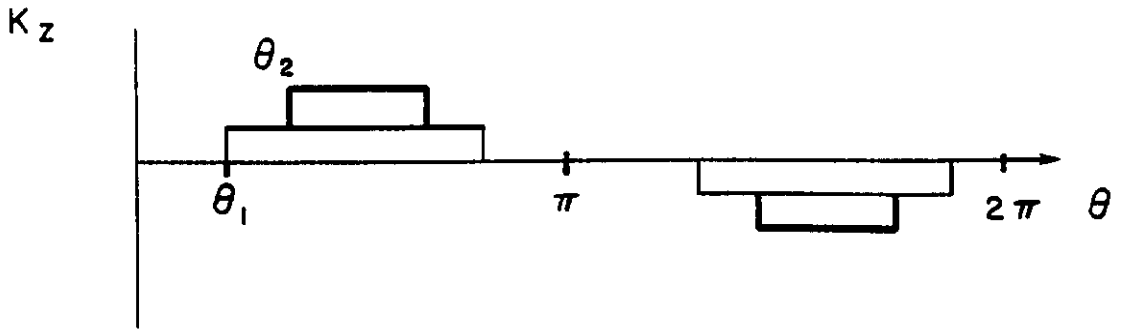

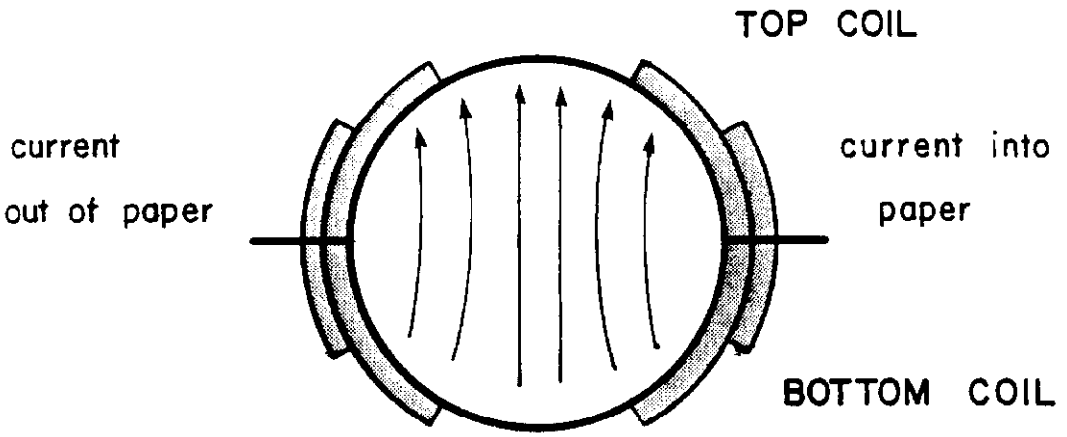

NOW HAVE TWO ANGELS θ_o θ_1
MAKES IT POSSIBLE TO ELIMINATE

m = 5	DECAPOLE	$\theta_1 = 12°$
m = 6	0 BY SYMETRY	$\theta_o = 48°$
m = 7	1st NON-ZERO TERM	

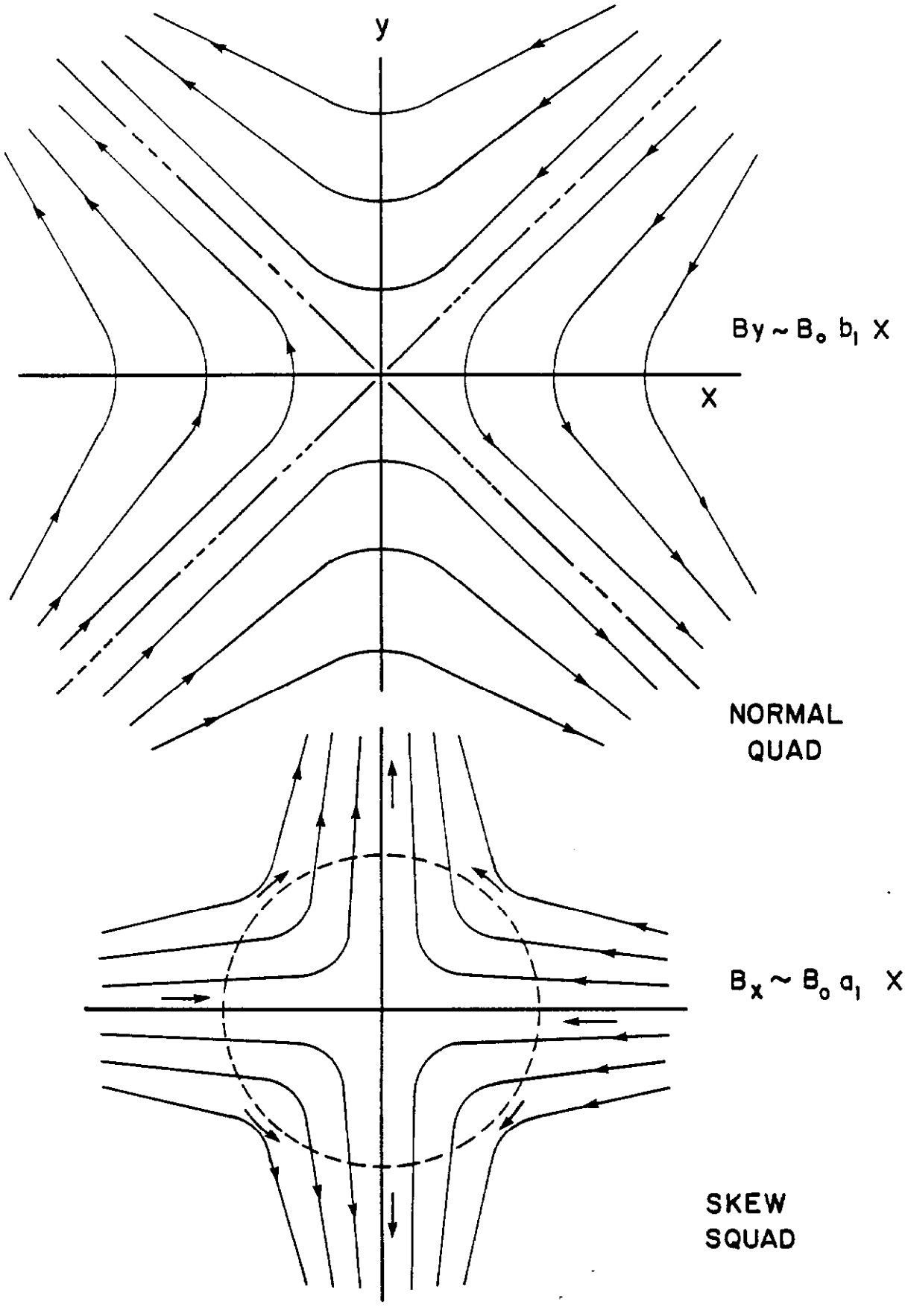

Projection 34

EXAMPLE OF 5' MODEL CALCULATED BY S. SNOWDON

$\int B\,dl.$ THRU MAGNET

X $\int B\,dl.$ NORMALIZED TO 1 AT X = 0

INCHES	
0	1.00000
.3	1.00001
.4	1.00002
.5	1:00003
.6	1.00004
.7	1,00005
.8	1.00002
.9	.99992
1.0	.99965
1.1	.99906
1.2	.99789
1.3	.99564
1.4	.99134
1.5	.98267

can be replicated easily by means of precision stampings. A little calculation shows that in general the conductors must be positioned to an accuracy of the order of 1/1000 of an inch. It should also be clear that the accuracy of the envelope is determined by the collaring structure that supports the coil. We are thus faced with a new problem in magnet construction, namely, we can get a given field provided we can hold the placement of the conductor to a sufficiently small tolerance. The first impulse is to try the solution shown in Projection 36. I call this approach the Old World Craftsmanship approach. Each coil is constructed with very high precision and very careful control. Maxwell's equations then guarantee that we will have the proper field. However, I feel that this is an analog computer for solving these equations, and it does not represent a viable solution for mass producing superconducting magnets for use in high energy machines. Rather, we need to apply modern control techniques to this problem. Figure 37 shows a block diagram of the new type of approach. In this case, there is a factory whose basic function is to take in all of the raw materials and produce a finished coil in a fairly reproducible fashion. We then measure the output of this factory using a warm bore magnet testing technique and feed the errors back into the factory in order to cancel out the noise. This is the system that has been developed at Fermilab. At present the feedback loop is not closed on an individual magnet. The test is made at the point when the coil is collared when about 1/3 of the cost has been invested in the magnet. If a coil is out of tolerance, te room temperature test will indicate the trouble, and the collars can be removed and the coil recollared. However, at present we are trying very hard to close the feedback loop with zero delay. The theory of this is explained in Projection 38.

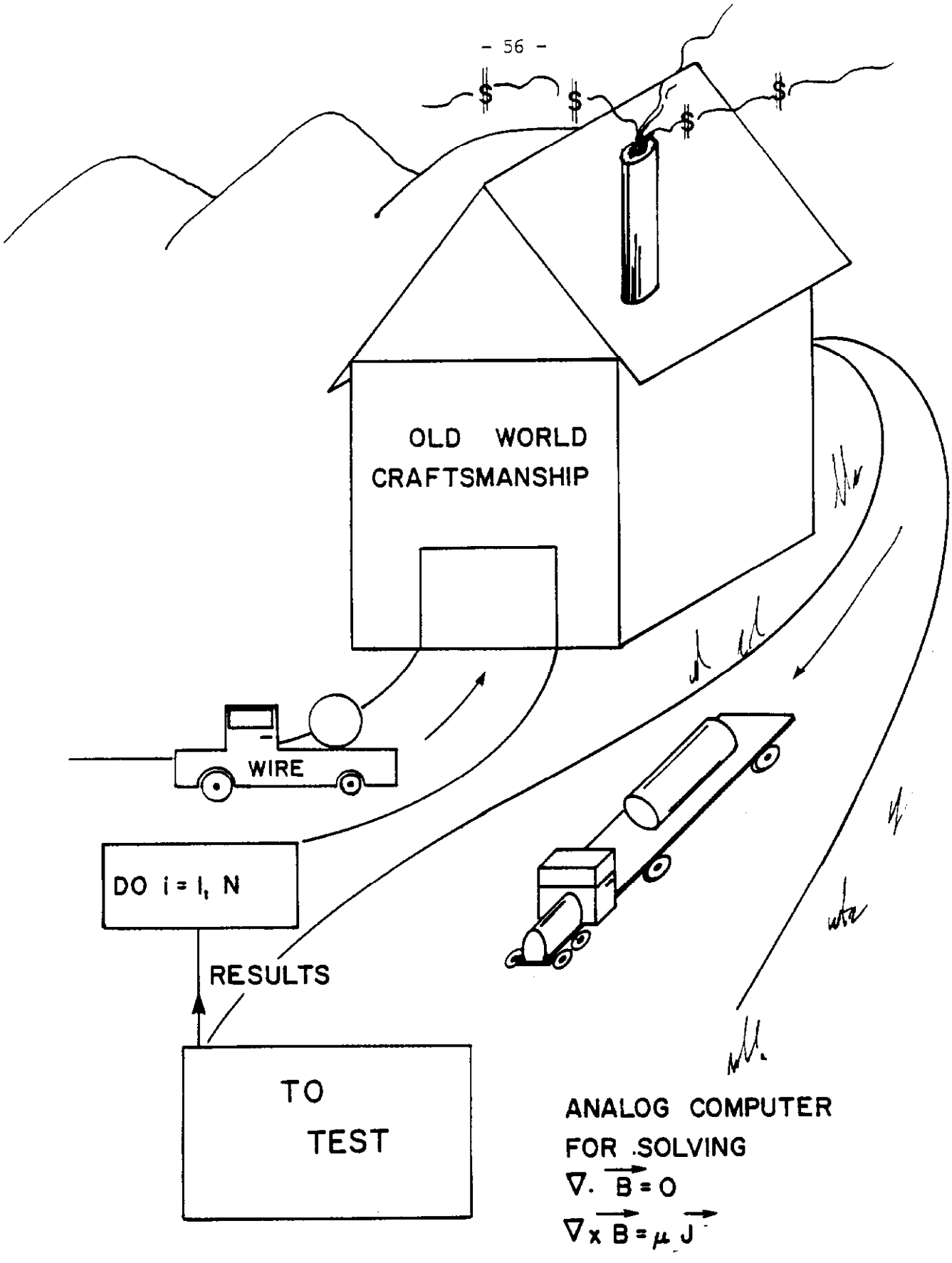

Projection 36

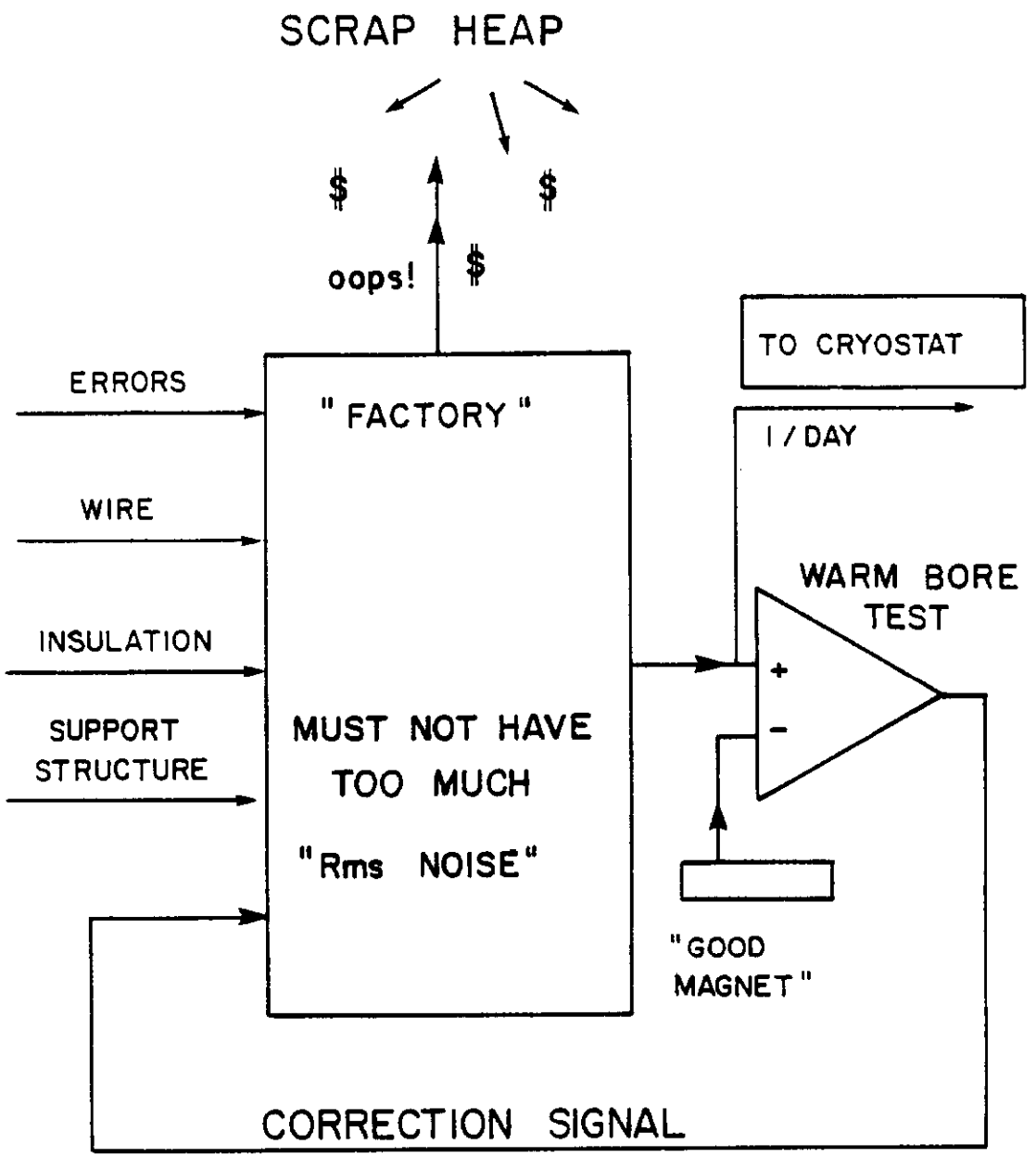

ANALOG COMPUTER FOR

"SOLVING GOOD MAGNET"

PROBLEM

I would like to comment a little bit on the philosophy that has been evolved for coil construction. Rather than controlling with great accuracy the shape of a coil, we have put a great deal of effort into building a machine that will make coils in a fairly reproducible manner. It does not matter if the coil is exactly round or if it is elliptical. Any nearby magnet shape will have an expansion in field harmonics of the type shown in Projection 32. The high harmonics will be mainly determined by the corners of the coil blocks. The magnet constructor has very little control over these things. The lower harmonics are determined by slow variations in the coil compaction. Figure 38 shows a perfect coil as a rectangular block and an actual conductor distribution that might be obtained out of such a production machine. The short term wiggles in this curve only couple into the high harmonics in a rather insignificant fashion. However, the gross variation couples into the lower 5 field harmonics and causes these coefficients to fluctuate. In fact, experience has taught us that the quadrupole, the sextupole, and octapole terms are the place where one has the main problems with field quality. However, the integrals that determine these coefficients are not only determined by the distribution of current over the block but also by the angle at which it is terminated. If one could measure these lower harmonics and then shim the individual coil blocks to have individually determined angles, one could correct the lower harmonics of the coil for any inaccuracy within the body of the winding. The Fermilab coils have just this feature. First of all, we use the room temperature measurement to emperically determine the distribution of wire in the body of the coil, and, secondly, we can control the

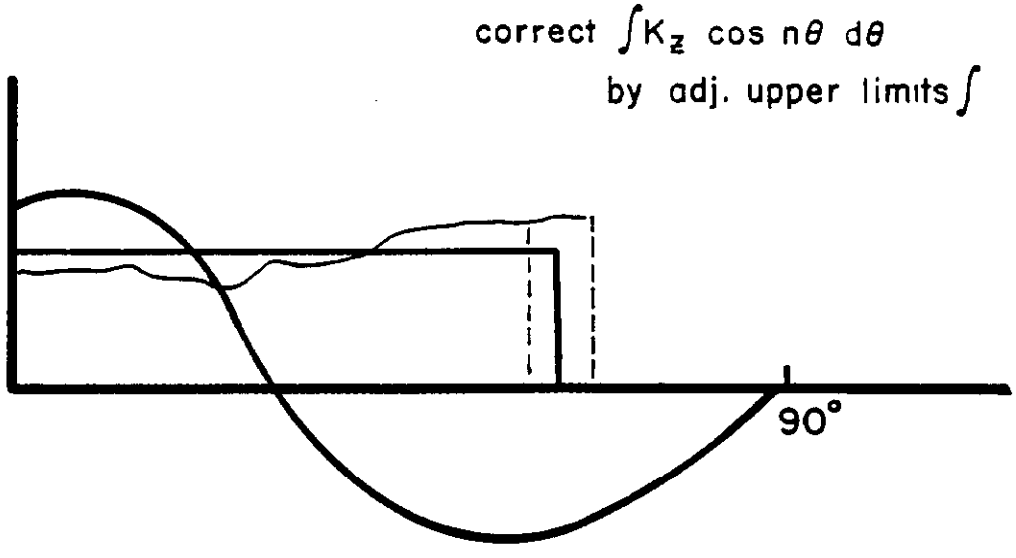

ELEMENTS NEC. FOR CONTROL LOOP

1- MEASUREMENT

2- CONTROL POINT. i.e. SHIMS

Projection 38

field by inserting shims as is shown in Projection 39 at the keys of the collar. There are 8 points where shims can be inserted and, consequently, there are 8 harmonics that can be corrected in the coil. At present, we are constructing a temporary collaring apparatus that will allow us to measure the normal and skew, quad and sextupole moments of the winding. This process will only take an hour or so and then individual shims can be placed in the magnet at the points indicated in order to individually correct a coil. When this system is in operation, it is anticipated that we will control the field to a few parts in 10^4.

There is a systematic source of field errors other than just errors in the winding. As mentioned previously, the forces in a coil are very large. These forces cause conductor motion and so a coil, even with perfectly placed conductors, would have a field that is dependent upon current. Projection 40 shows the forces on individual conductors in one of the Fermilab magnets. In addition to the forces shown in cross section, there is an axial force of 16,000 lbs. which lengthens the coil by about .07 in. during pulsing.

Projection 41 shows the azimuthal force as a function of conductor number for the inner and outer winding of our magnets. It is seen that the force is almost linear with conductor number. The force is largest at the high field near the top key of the inner winding. Let us now calculate the effect of this force on the conductor. To do this to the accuracy required at this point, does not involve using a big computer and a "finite element" stress analysis program. We can get a good feeling for the problem by the following simple model.

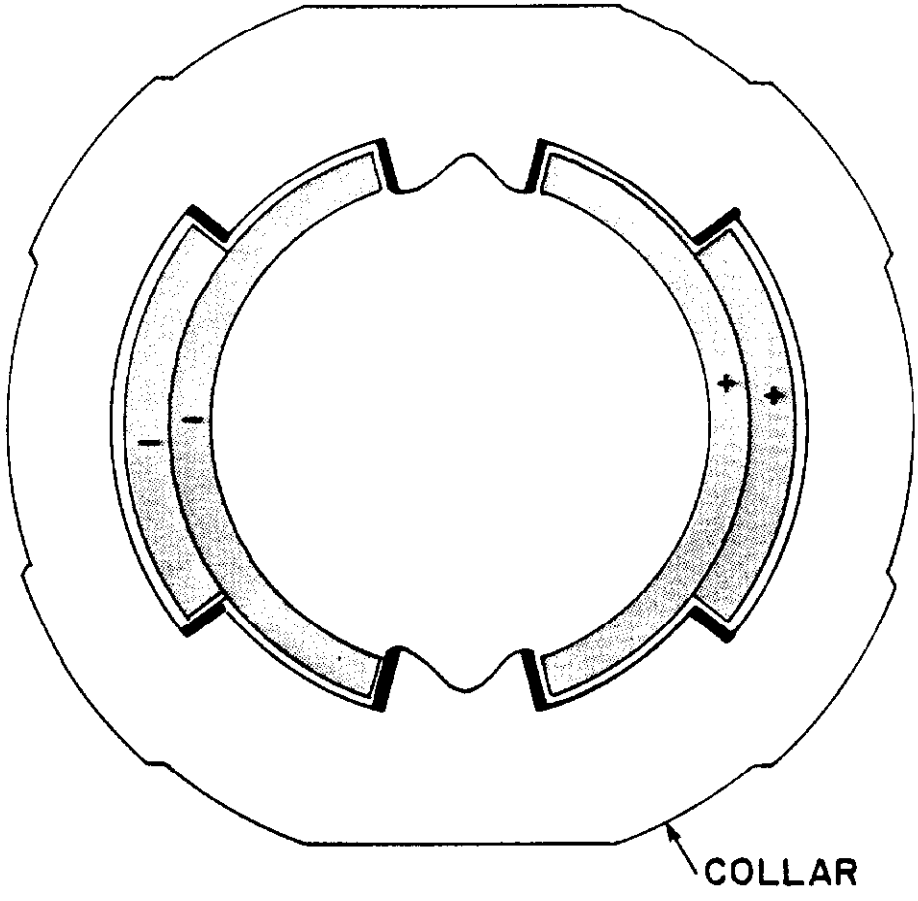

SHIM

COIL

ADJUST SHIMS TO GET PROPER FIELD
IN PRODUCTION MAGNET

Projection 39

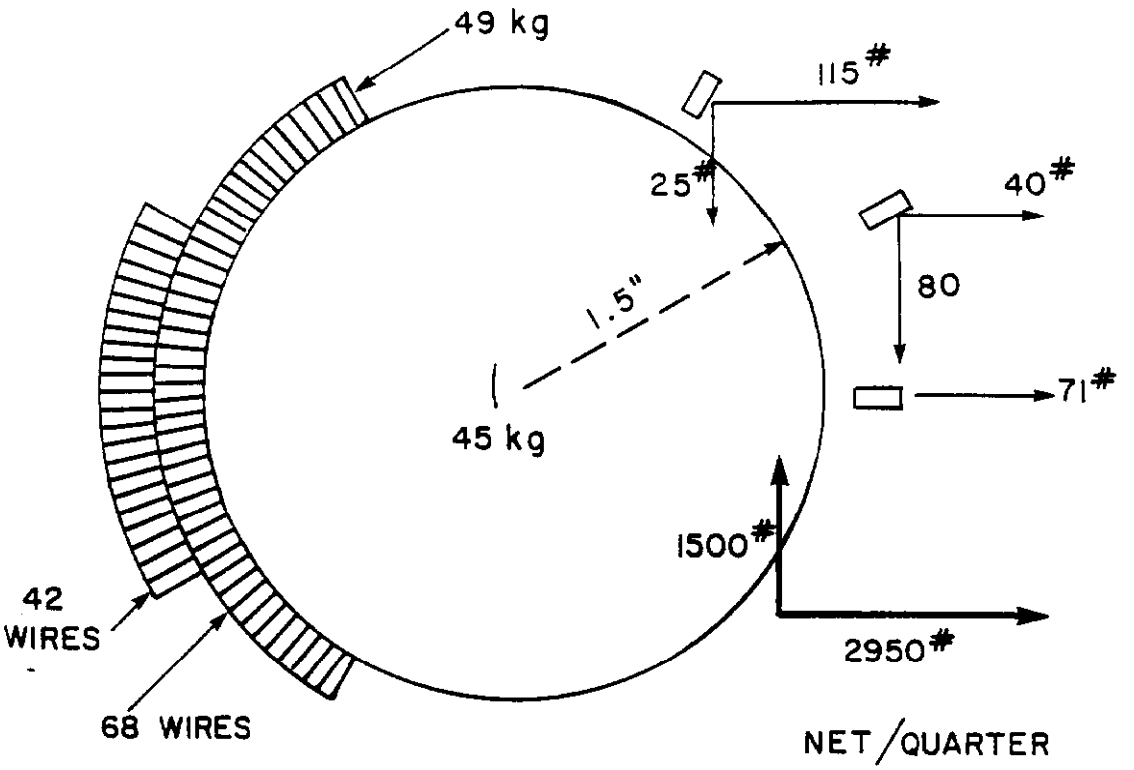

FORCES AND FIELDS IN A
SERIES E MAGNET

$$\text{Axial Force} = \frac{\partial}{\partial z}\left(\tfrac{1}{2} L I^2\right)$$

$$= 16000\ \#$$

Projection 40

Projection 42 shows the winding as a series of springs. The one end is at the key and is fixed, and the other end is the centerline or the midplane of the magnet winding and is fixed by symmetry. The forces shown as p_i are linear azimuthal forces shown in the last figure, and the spring constant represents the combined elastic constant of the cable plus the insulation matrix. We can linearize the problem and treat the springs as though they had a fixed constant k. We will treat p_i as proportional to i, the conductor number. The difference equation can be solved, and it gives a displacement Δx_i as a cubic function of the conductor number. The maximum displacement occurs a little bit past the center of the winding.

However, the main point for solving this problem is to find out the preload necessary in the spring in order to keep the end of the coil near the key in contact with the key when the coil is magnetized. This force for our magnet turns out to be about 1500 per linear inch of length of conductor. The resulting motion for a Youngs modulus of the matrix of about 10^6 lbs./cm is about 2-1/2 mils maximum and is shown at the top of Projection 43.

In addition to this elastic motion of the winding, there is also an elastic motion of the coil collars. This is shown in the bottom of Projection 43. The circular collars distort into a slightly elliptical shape. The diagram shown is much exaggerated. The point at 45 does not change in radius but moves in azimuth. The points at the pole and the equator do not move in azimuth but move in a radial direction. We thus have altogether three motions of the wire that combined to make field errors. These motions all are proportional to B^2 in their magnitude. The amplitude of them at 40 kG

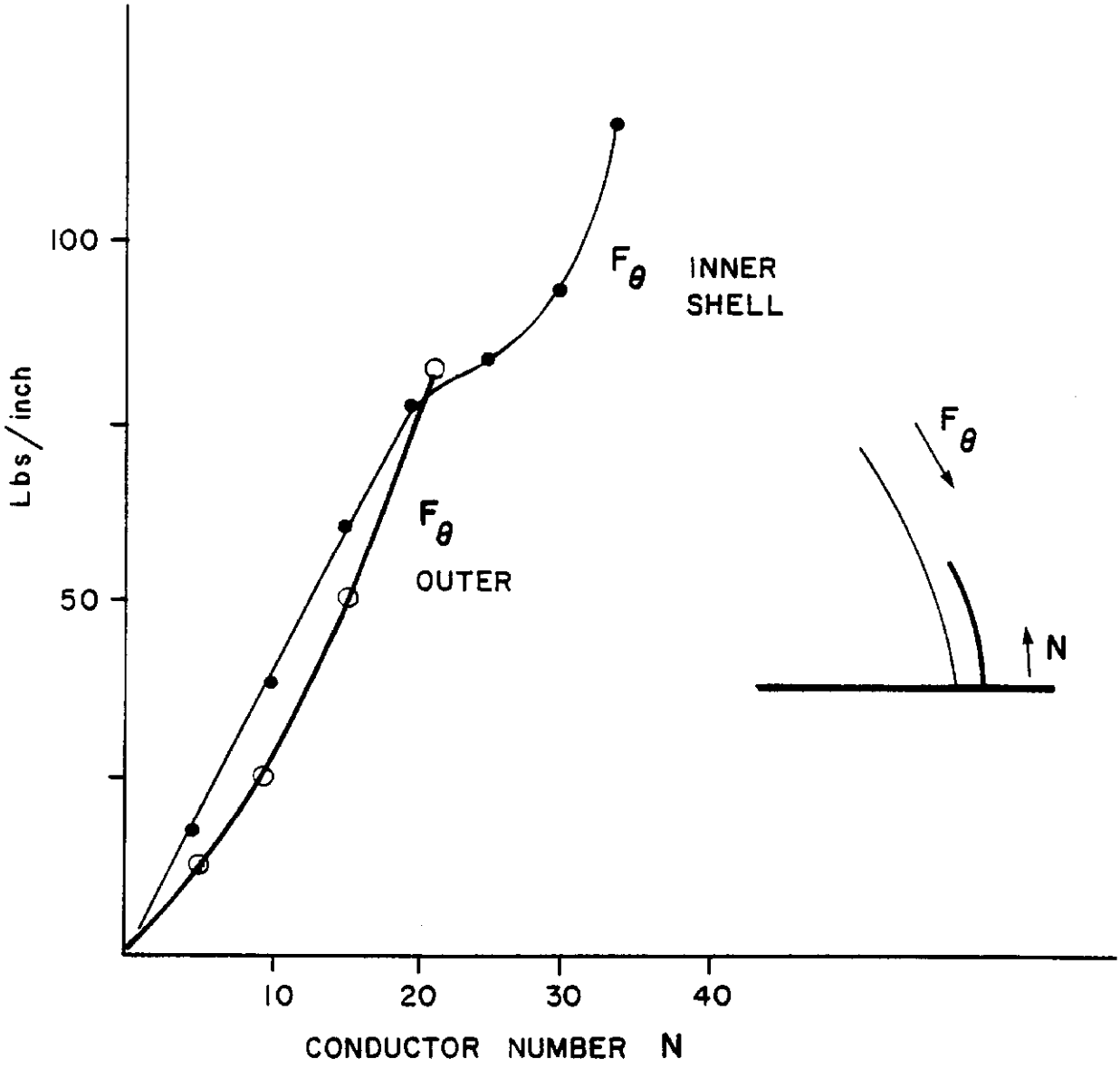

Projection 41

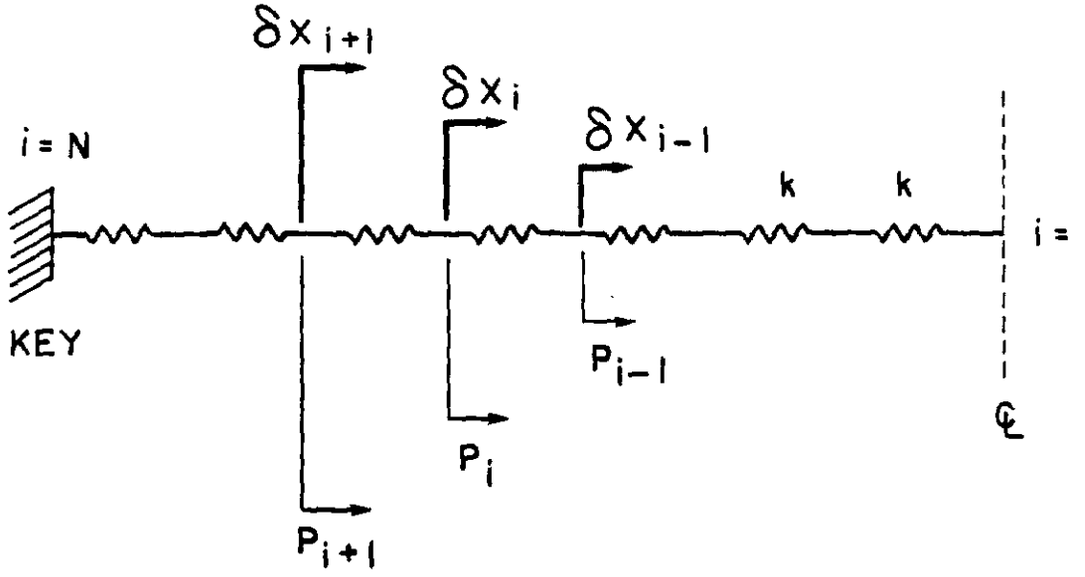

Linearize : $P_i = \alpha i$

Spring has linear constant k

$$\delta X_{i+1} - 2\,\delta X_i + \delta X_{i-1} = \alpha i$$

Solve

$$\delta X_i = -\frac{\alpha}{6k}\,(i-1)\left[(i+1)\,i - (N+1)\,N\right]$$

MAX X_i at

$L_m = \sqrt{1/3\,(N^2 + N + 1)}$ → gives X max

GET Prelood from spring at end

$$F = k\,\delta X_{N-1} = 1/3\,\alpha(N-2)\,N \approx 1500\,\#$$

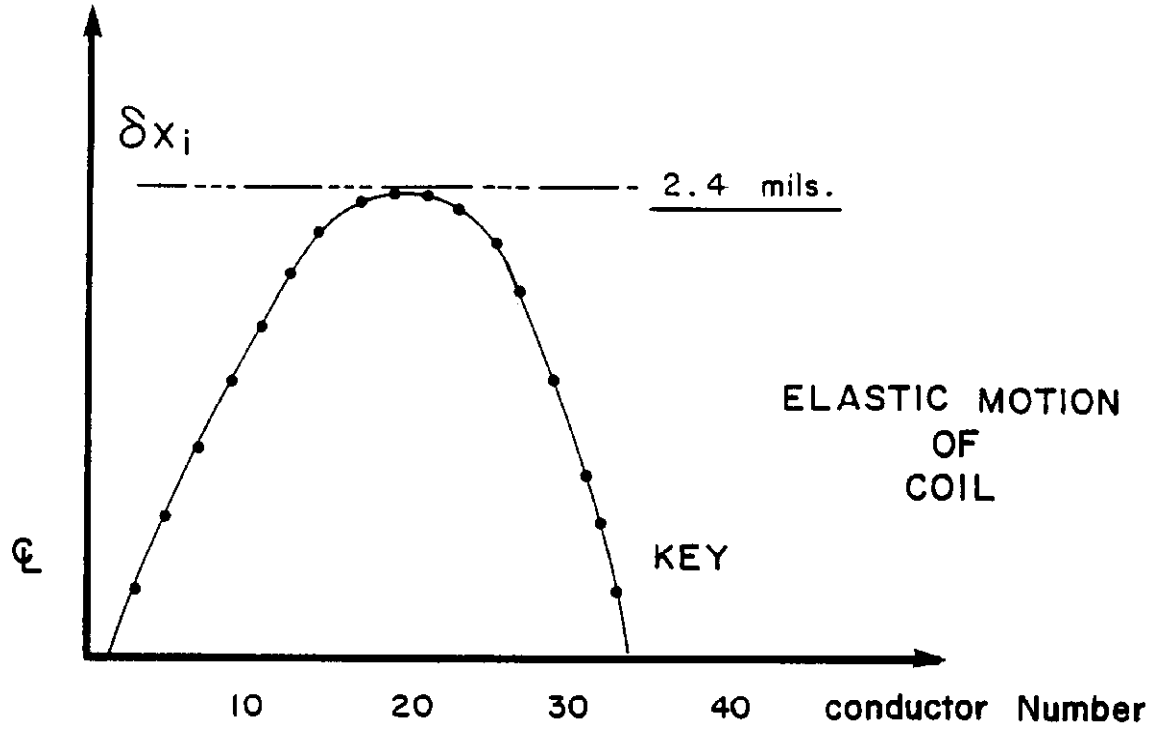

COLLAR MOTION

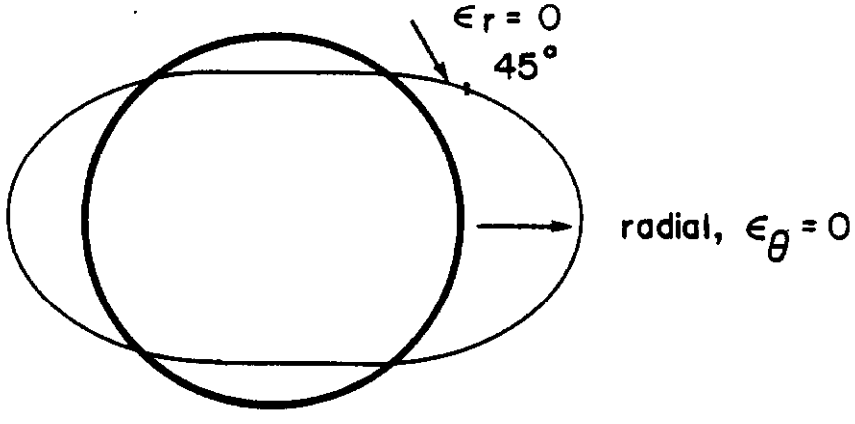

δx , ϵ_r , ϵ_θ make FIELD errors

$$\frac{\delta B}{B} \sim I^2$$

is shown in Projection 44. ε_θ and ε_r are due to the collar motion. The direction of these curves can be understood as follows: ε_θ compacts the winding more to the equator and, hence, makes the field stronger as one goes toward the winding. ε_r moves the winding away from the axis and, hence, causes the field to fall off. The detailed mechanics of the collars connect ε_r and ε_θ. If the collar was a uniform ring, ε_r would be twice ε_θ. The sum of the above terms is shown in the bottom of a figure and for a comparison, the amount of sextupole necessary for chromoticity correction, if it were distributed uniformly throughout the dipoles, is shown as a dotted curve. This is only shown to give one some feeling for the magnitude of the error fields involved.

The point I would like to make here is that there are many reasons that correction coils are necessary in a superconducting machine. The persistent currents must be corrected, and their major component is a sextupole term. In addition, as we have just seen, conductor motion causes a distortion of the winding during pulsing, and finally, the residual of the iron yoke must be corrected, and a chromoticity term must be added. They must also provide correction fields over the whole range of magnet operation. This indicates that the correction circuit problem needs much more attention in a superconducting machine than it has received in past machines.

I would now like to address a problem that has caused and is causing an enormous amount of difficulty. This has to do with the subject of preload. Whatever scheme is used for confining the coil, the mechanical forces must exceed the magnetic forces or the coil will move away from the support form. Once this happens, the quality of the magnetic field deteriorates rapidly.

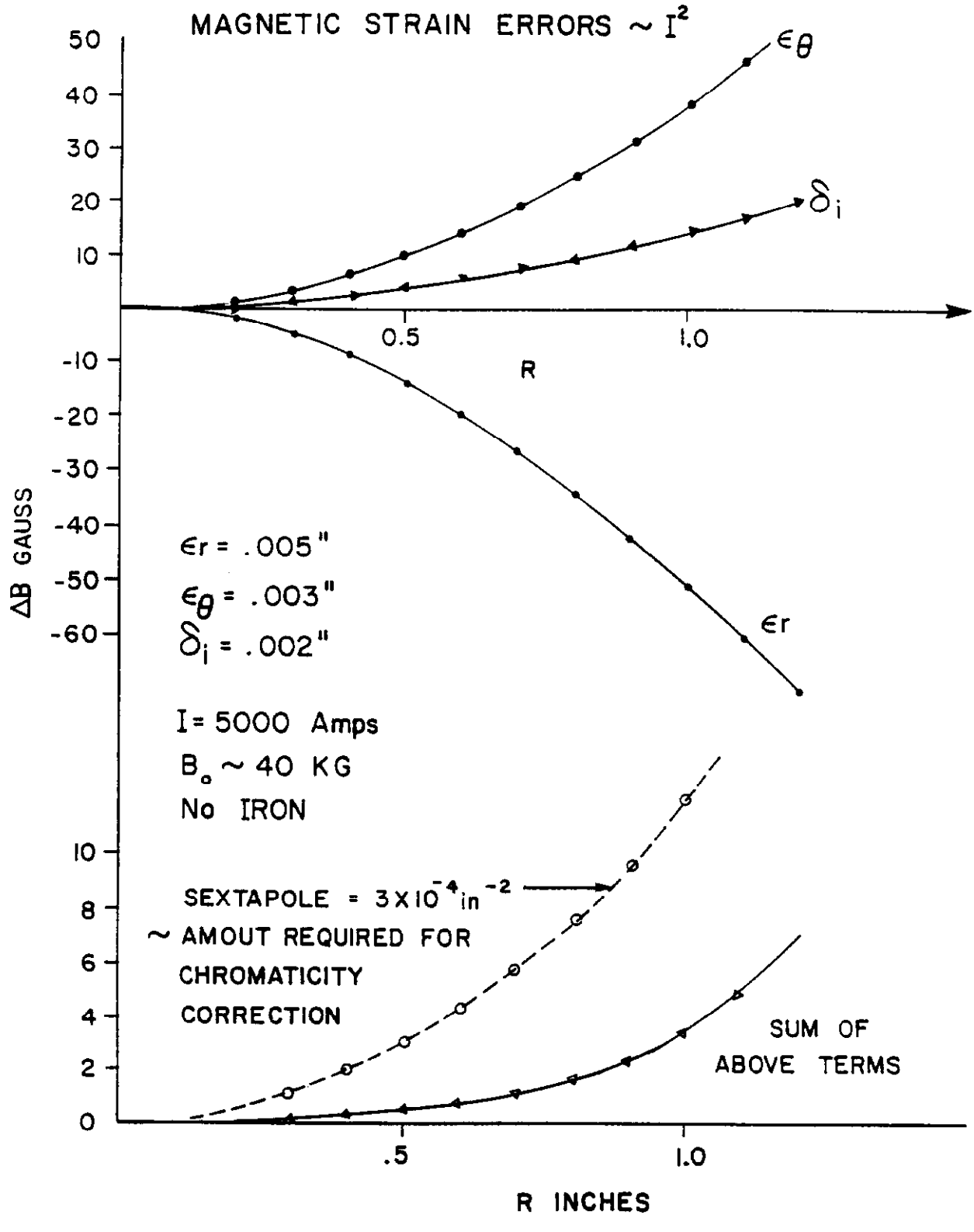

Projection 44

In addition, we have seen in the first part of the discussion that the situation can lead to excessive training or the coil not reaching its short sample limit. However, there is a nasty reality that must be faced here. The coil when it is cold shrinks away from the collars. Thus, the stress in the coil at room temperature is much bigger than it is when it is cold. Projection 45 shows a typical situation that we have encountered at Fermilab. The coil size is shown along the horizontal axis, and the force applied is shown along the vertical axis. The open loops represent the stress strain diagram for the coil matrix. When the coil is cooled, it shrinks relative to the collar and winds up at the point indicated on the drawing as "preload." This preload must be greater than the magnetic forces or the conductor will move away from the confining collar. Thus, one can see that the more coil shrinks relative to the collar, the more it must be compressed at room temperature in order that the proper preload will exist when it is cold. The details are shown in Projection 46. There doesn't have to be a solution to this problem if the coil shrinks too much relative to the collar. It could easily happen that the matrix crushes before a sufficient preload at room temperature could be applied. We do not know how to control the mechanical properties of the insulation matrix, and research needs to be done on this subject.

Projection 47 and 48 show some of the areas that we need to investigate.

Fatigue Stability

1. Coil support. We do not know how to build a satisfactory support structure for a 10 Tesla coil. Much work needs to be done on this subject.
2. The mechanical properties of the insulation and its aging under many magnetic cycles is not understood.

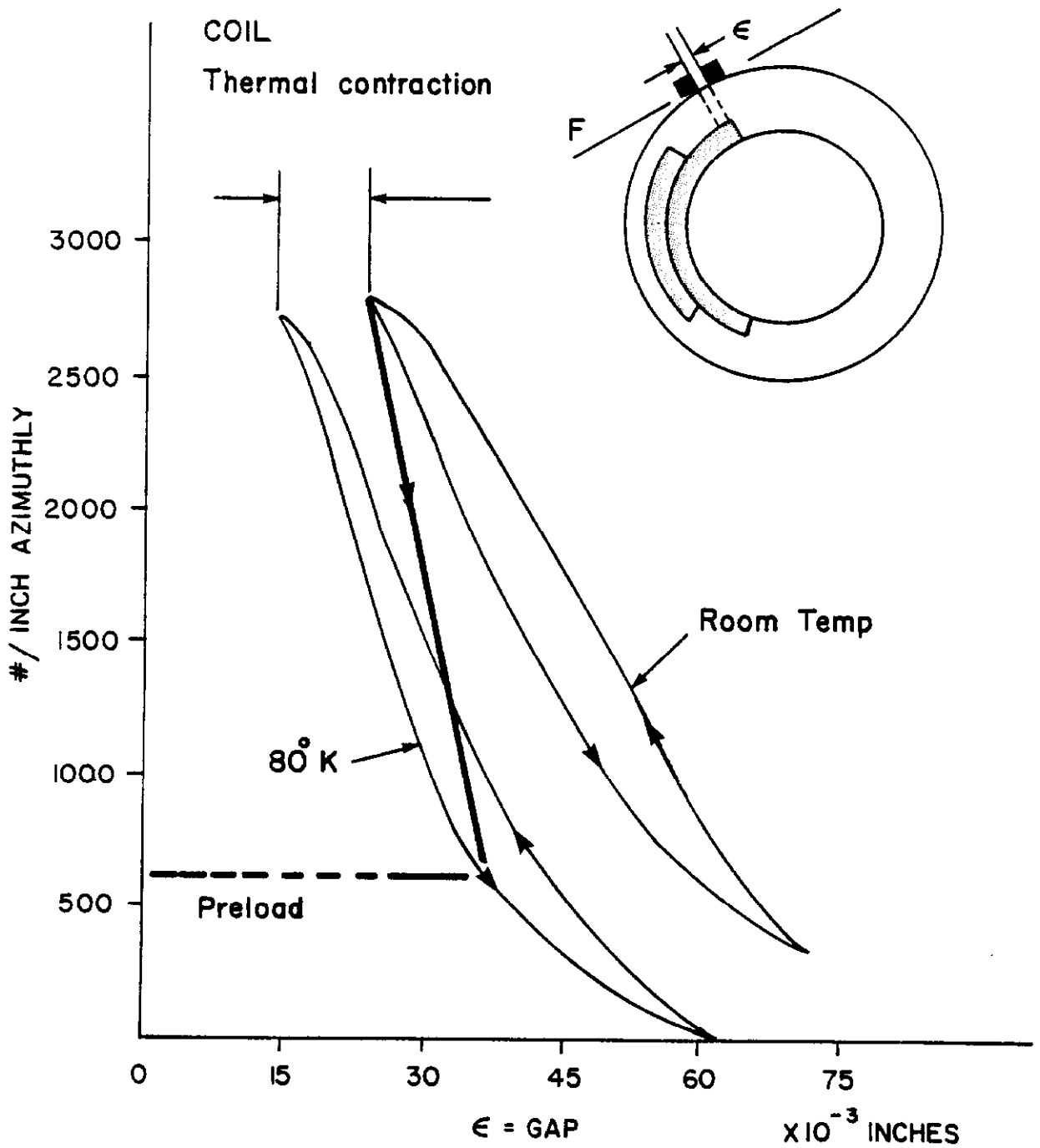

Projection 45

PRELOAD PROBLEM

1 - Coil shrinks

2 - Collar shrinks

COLLARS SS
Gloss epoxy coils

If 1 > 2 Lose preload

If 2 > 1 Gain preload

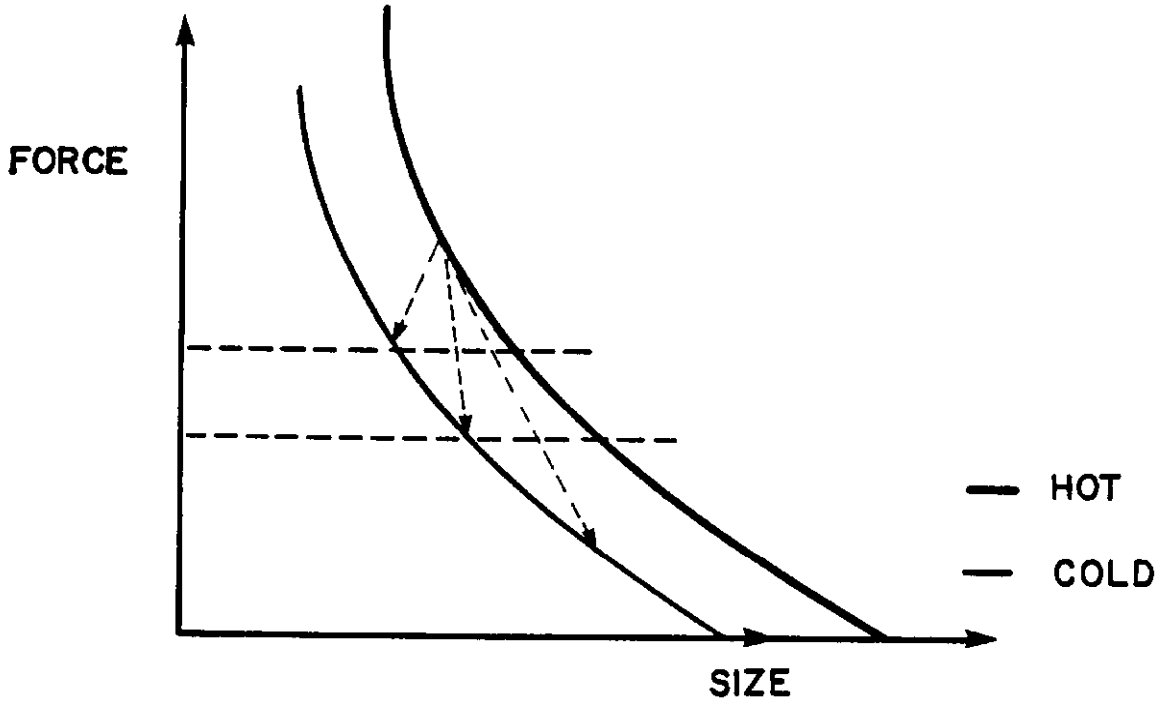

DETECT Preload = 0

b_2 , b_4 change with I

3. The cryostat is also subjected to both thermal stress and magnetic stress. Work needs to be done on this subject.
4. It is not known whether stainless steel at high stress, low temperatures, and high fields is stable.

Matrix

5. At Fermilab the support matrix has some of the properties of styrofoam, namely, it crushes inelastically after a certain force is applied to it. It behaves elastically around the permanently deformed position. This leads to easy assembly of the coils. This solution is probably not applicable at the 10 Tesla level.
6. One can imagine strengthening the support matrix by impregnating the epoxy with aluminum oxide or glass. We tried this as an experiment once, and it leads to an exceedingly stiff coil. Glass may be necessary if one goes to Nb_3Sn conductor.
7. In addition to supplying support, the matrix has to provide adequate insulation and guarantee that there are no turn-to-turn shorts. This represents a wide area that needs study.

Cryostat

8. Cryostats need more research on them. The mechanical support that the cryostat must provide is such that the magnet vertical axis needs to be stable to a mrad, and the X and Y position of the quadrupoles stable to 20 mils or better. This, in spite of rather large mechanical deformations. The Fermilab magnets shrink about 3/4 in. between room temperature and liquid helium temperatures. The behavior of superinsulation in a large cryogenic system needs to be studied. How stable is the infrared reflection coefficient of superinsulation?

9. How does one counter the thermal stresses in a cryostat?

10. And how does one find leaks in a large system?

11. How does one rapidly warm up a system and change a magnet?

12. And the question of high current leads needs to be studied more.

Quality Control

13. Finally, the question of quality control needs to be studied in much more detail. We have made tremendous strides in this field, but we have consistently underestimated the care that must be exercised to build a superconducting magnet.

Systems

How does a large system of magnets behave? At Fermilab, we have three areas where the behavior of strings of superconducting magnets is being studied. The first is the program at B12 which is above ground and involves a string of 16 magnets and their associated quadrupoles. It represents as closely as possible the conditions that will be found in a string of magnets in the tunnel. Quench protection techniques are being studied. Failure modes of systems of magnets will also eventually be studied in this area. So far the string has been pulsed to about 3,000 amps and quenched safely. The pressure rise in the cryostats under quench conditions and the behavior of the cooling system for the magnet string is also being investigated.

There are also two strings of magnets installed in the tunnel. One has been cooled for more than a year, and the second one is just now starting to cool down. What problems can arise in a system of magnets?

First of all, each one of our magnets stores about 350 kJ. If a magnet quenches, its terminals are shorted by an SCR, and an internal heater is fired in order to drive the magnet normal as fast as possible. The energy

RESEARCH

FATIGUE STABILITY

1- Iron support $F \sim B^2$ 10T

2 - Insulation 6X FORCE

3 - Cryostat (Thermal cycles)
(Magnet Forces)

4 - Stainless Steel

a) Hi stress

b) Low Temperature

c) Hi Fields

MATRIX

a- "Styrofoam" Easy essembly
Self correction
Does it extrapolate
To high field

b - Al_2O_3 + epoxy

Glass

What about Nb_3Sn

c - Electrical insulation

CRYOSTAT

1- Mechanical Support

$\theta \sim 1$ mr

X, y ~ .02"

2 Termal Stresses

3- Leak testing !

4- Hi Current lead.

Manufacture

QUALITY CONTROL TECHNIQUES

from the nonquenching magnets is extracted and dissipated in an external resistor. Brookhaven and Fermilab have evolved two different schemes for protecting their magnets. In each case, the full energy within a magnet is dissipated in the conductor.

To understand how this works, consider Projection 49. Here we show a piece of the conductor going normal and generating a quantity of energy given by I^2rdt. If we neglect the helium cooling, this heat has to result in a temperature rise to the material which is equal to cdT. We can rewrite the equation as shown in the second line. The heat capacity and the resistance as a function of temperature are known, hence, the right side of the equation can be numerically integrated and is only a function of the final temperature. Thus, for a given final temperature, there is a fixed $\int I^2dt$ the conductor can tolerate. We have made detailed measurements of this property of the conductor and find that at high currents the helium cooling can indeed be neglected, and the curve shown in Projection 50 for the temperature as a function of $\int I^2dt$ is quite accurate. One can check this by exposing the conductor to a given $\int I^2dt$ that should take it to the melting point of either Stabrite or Mylar. These two substances give a calibration point at about 600° K.

The magnet protection system must always keep the $\int I^2dt$ below some value set by the designer. Since the conductor has to absorb all of the energy in the magnet, one can lower the average by driving all of the conductor in the magnet normal at once. BNL does this by causing the quench to propagate by thermal conduction over a large number of turns in the magnet. At Fermilab, we apply an active quench protection system, and we actually activate a

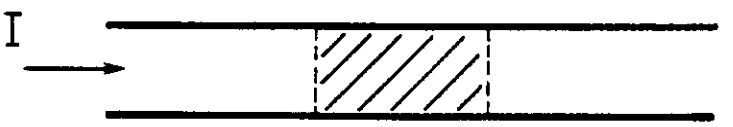

$I^2 R\,dt = C\,dT$ if He disregarded.

$$\int_{t=0}^{t} I^2 dt = \int_{T_i}^{T_f} \frac{C(T)}{R(T)}\, dT$$

↑ known

For Short Times

$$T \sim t^{1/3}$$

For Long Time

$$T_{MAX} \sim e^{I^2}\ !$$

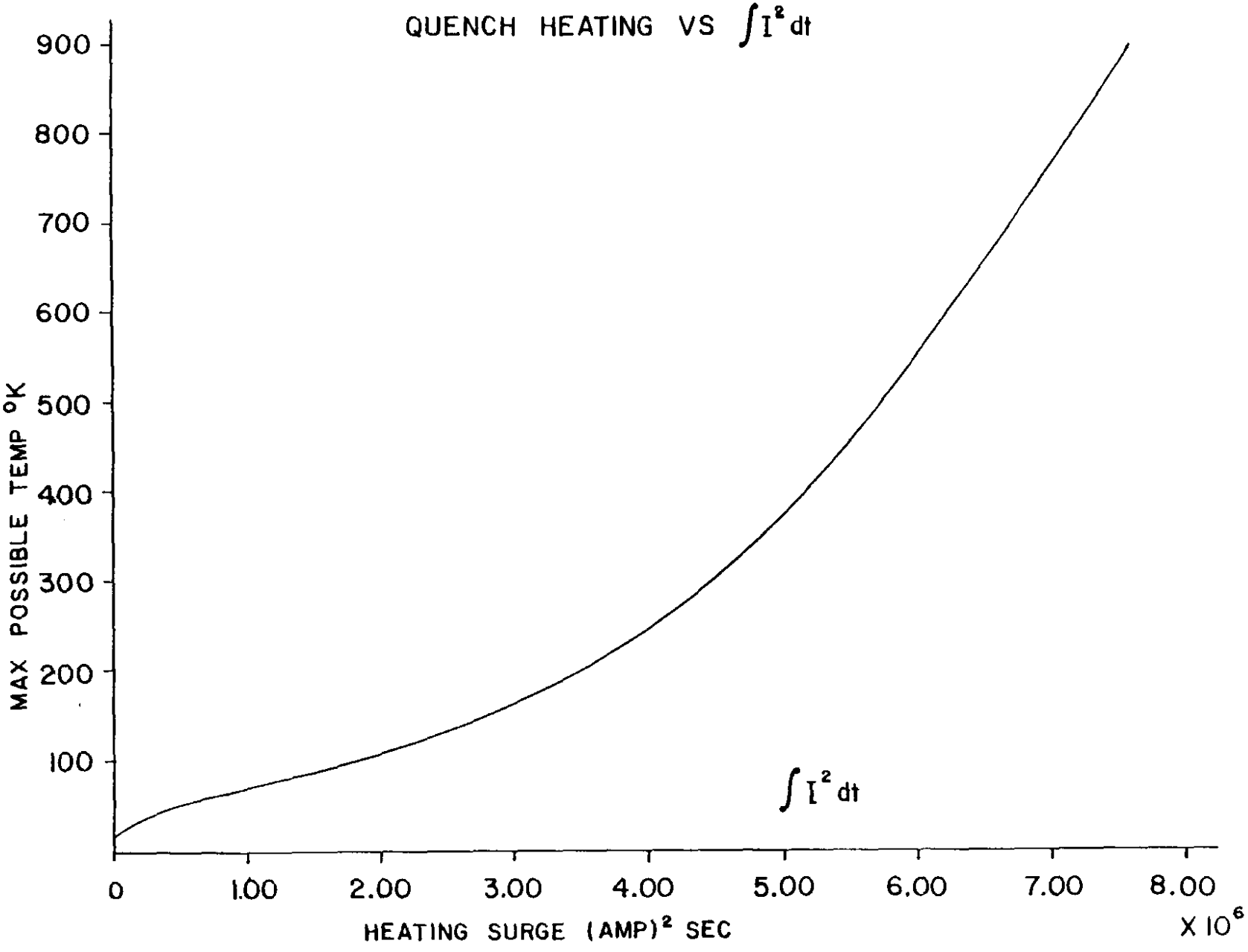

Projection 50

heater in contact with the turns in order to spread the quench over a large region of the magnet. Once enough conductor turns normal, the resistance becomes large, and the time constant to discharge becomes short. Thus, the $\int I^2 dt$ is limited. The Fermilab magnet protection scheme holds the $\int I^2 dt$ to about 5×10^6 amps^2/sec. It should be noted that as Projection 49 shows, T_{max} varies like an exponential of $\int I^2 dt$, so this quantity must be carefully controlled.

When a magnet quenches, abnormal voltages appear across the turns. In order for the magnet to survive is the voltage between turns must not become large enough to cause breakdown. Helium is not a very good insulator in its gaseous form. Projection 51 shows some emperical breakdown data for the Fermilab type conductor as measured at various temperatures in helium. Additional data that has been measured is shown in Projection 52. It is safest to disregard the properties of helium as an insulator and insure that the conductor is adequately insulated by some material such an mylar in order to guarantee that there will not be shorts when the magnet quenches.

Another problem that will be encountered in large systems is the radiation quenching of the magnets by any beam that manages to hit them. Some measurements have been made on Fermilab magnets, and these appear in the Tevatron Design Report. I show two examples in Projection 52. Two cases were studied:

1. A fast beam loss, such as that would be encountered in slow extraction.
2. A slow beam loss, as would be encountered in slow extraction of the beam, for example for use in the Meson Lab.

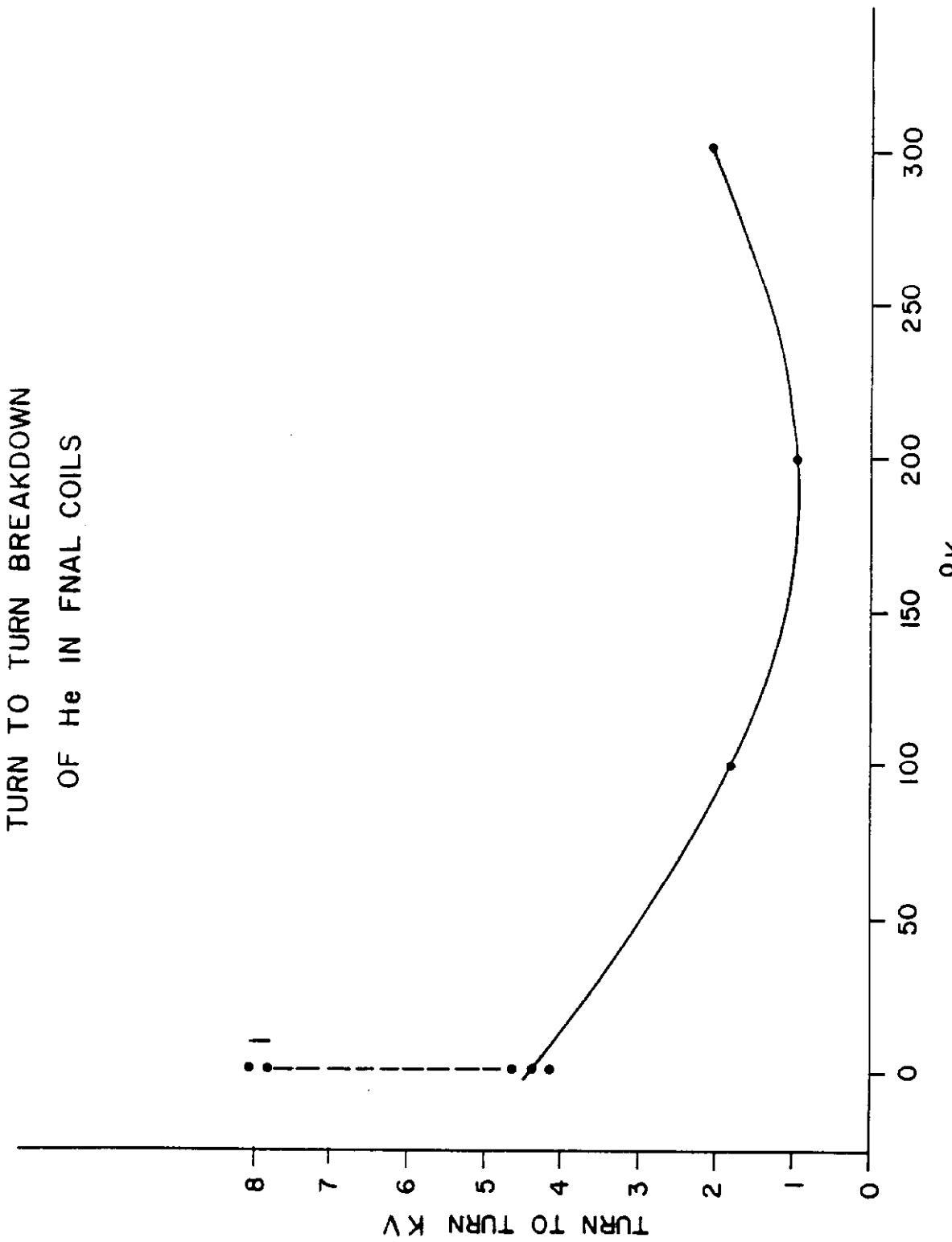

Projection 51

How well we can control these loss mechanisms will control how close we can operate the machine to the short sample limit. A great deal of work needs to be done in this area yet.

Let me summarize here some of the systems problems that we are going to have to cope with. I have already mentioned the quench protection systems are passive at BNL and active at Fermilab. I think a question remains of how active the system should be. In the Fermilab case, a microprocessor is monitoring the magnet behavior. The next level of sophistication above protecting the magnets would involve monitoring the cryogenic part of the system and minimizing the perturbation to the refrigeration.

The cooling system is unique because a synchrotron is spread out over a large area and is very complicated with many parallel paths. The system needs to be brought under computer control. There are some special problems that arise because when the system is pulsed, a large heat load is added through the eddy current and hysteresis loss in the magnets. In the Fermilab case, this results in a large evolution of gas which must be handled by the refrigeration system.

We desperately need new leak detection systems and ways to isolate leaks in the complicated cryostats that house the magnets. We need to study how to get fast access to the magnets in order to change them if one is damaged. We need to understand for the future the behavior of superfluid helium in large systems.

Power supplies will need additional development. The long spills that are possible with the superconducting system can change the proton economy.

Long spill times mean that the secondary beams will become major users of protons. In the past, the counting rate has set a limit to the number of protons that could be utilized in these beams. Long spills involve very stable power supply systems.

Correction coils will demand much more complicated programs and more sophisticated power systems in order to correct the field dynamically. In the past, the main burden of good field has been placed upon the dipole magnets, and this good field has been determined by iron stampings. This is no longer true, and indeed, in the future it could become very expensive to place the main burden for good field on the dipoles. The correction coils must be considered as part of the economic equation. It may well be less expensive to concentrate more on the correction circuit and less on the quality of the dipoles.

Finally, as I have mentioned, we need much more work on understanding the interaction of radiation on the magnet system.

Conclusion

I would like to conclude this talk by summarizing shortly our situation. We have not made very much scientific progress in understanding training and the quenching phenomena that take place in our magnets. In order to take the next step and go to a 10 Tesla magnet, much work needs to be done. The support matrix must be understood in detail, and the black magic turned into a science. We need to understand the action of HeII on the cooling system, and in order to go to higher field magnets, we may well have to develop new techniques to form Nb Sn in situ. We have made great strides in understanding the role of quality control in the construction of magnets and understanding the

manufacturing process that will economically construct useful magnets. We are on the verge of obtaining much information about systems of magnets and how to control them, and I feel we are making great strides in this field. It seems inconceivable to me that only five years ago we were still building 1 ft. model magnets at Fermilab. However, it is still true that many interesting and vexing questions still remain.

Many of my colleagues at Fermilab were involved in collecting the information I have discussed. Their names can be found in the appended Bibliography.

Finally, the great influence of Dr. R. R. Wilson can be seen throughout the FNAL work.

Fermilab

March 24, 1980
Section 1

BIBLIOGRAPHY

ENERGY DOUBLER DIVISION PUBLICATIONS - 1979

"Progress Report - Fermilab Energy Doubler", A. V. Tollestrup, IEEE Trans. Magn., MAG-15, No. 1, 647 (Jan. 1979).

"Fermilab Doubler Magnet Design & Fabrication Techniques", K. Koepke, G. Kalbfleisch, W. Hanson, A. Tollestrup, J. O'Meara, J. Saarivirta, IEEE Trans. Magn., MAG-15, No. 1, 658 (Jan. 1979).

"The Support & Cryostat System for Doubler Magnets", G. Biallas, J. E. Finks, Jr., B. P. Strauss, M. Kuchnir, W. B. Hanson, E. Kneip, H. Hinterberger, D. DeWitt, R. Powers, IEEE Trans. Magn., MAG-15, 131 (Jan. 1979).

"Room Temperature Field Measurements of Superconducting Magnets", R. E. Peters, L. Harris, J. M. Saarivirta, A. V. Tollestrup, IEEE Trans. Magn., MAG-15, 134 (Jan. 1979).

"A Superconducting Synchrotron Power Supply & Quench Protection Scheme", R. Stiening, R. Flora, R. Lauckner, G. Tool, IEEE Trans. Magn., MAG-15, No. 1, 670 (Jan. 1979).

"Superconducting Correction Elements", M. Leininger & F. Kircher, IEEE Trans. Nucl. Sci., NS-26, No. 3, 3931 (June 1979).

"Power for the Fermilab Tevatron Helium Liquefier", J. Hoover, J. R. Orr, J. Ryk, A. Visser, IEEE Trans. Nucl. Sci., NS-26, No. 3, 3938 (June 1979).

"How to Mass Produce Reliable Cryostats for Large Particle Accelerators", B. P. Strauss, G. Biallas, R. Powers, IEEE Trans. Nucl. Sci., NS-26, No. 3, 3941 (June 1979).

"Process Control System for the Tevatron Liquefier", H. R. Barton, Jr., et. al., IEEE Trans. Nucl. Sci., NS-26, No. 3, 4099 (June 1979).

"Central Liquefier for the Fermilab Tevatron", M. Price, R. Rihel, R. J. Walker, et. al., IEEE Trans. Nucl. Sci., NS-26, No. 3 (June 1979).

"Doubler-Tevatron μP Quench Protection System", R. Flora & G. Tool, IEEE Trans. Nucl. Sci., NS-26, No. 3 (June 1979).

"Beam Detector Assembly for the Fermilab Energy Doubler", E. Higgins, Jr., T. Nicol, IEEE Trans. Nucl. Sci., NS-26, No. 3, 3426 (June 1979).

"The Multiple Magnet Test Program", R. Flora, M. Kuchnir, et. al., IEEE Trans. Nucl. Sci., NS-26, No. 3, 3888 (June 1979).

"Pressure Development During Energy Doubler Quenches", M. Kuchnir & K. Koepke, IEEE Trans. Nucl. Sci., NS-26, 4045 (June 1979).

"Recent Measurement Results of Energy Doubler Magnets", M. Wake, D. Gross, M. Kumada, D. Blatchley, A. V. Tollestrup, IEEE Trans. Nucl. Sci., NS-26, No. 3, 3894 (June 1979).

Fermilab

ENERGY DOUBLER MAGNET DIVISION PUBLICATIONS - 1978

"Fermilab Experience on Large Superconductor Purchases and Its Implication to the Fusion Program", B. P. Strauss, R. H. Remsbottom, and R. H. Flora, Proceedings of the 7th Symposium on Engineering Problems of Fusion Research, IEEE No. 77CH1267-4-NPS (Jan. 1978).

"Production Test of Energy Doubler Magnets", R. Yamada, M. E. Price, and D. A. Gross, Adv. Cryo. Engr., Vol. 23 (1978).

Fermilab

December 28, 1977

1977 PUBLICATIONS LIST - ENERGY DOUBLER GROUP

"The Technology of Producing Reliable Superconducting Dipoles at Fermilab", W. B. Fowler, P. V. Livdahl, A. V. Tollestrup, B. P. Strauss, R. E. Peters, M. Kuchnir, R. H. Flora, P. Limon, C. Rode, K. Koepke et. al., IEEE Trans. Magn., MAG-13, No. 1 (Jan. 1977).

"Results of the Fermilab Wire Production Program", B. P. Strauss et. al., IEEE Trans. Magn., MAG-13, No. 1 (Jan. 1977).

"Measurements of Magnet Quench Levels Induced by Proton Beam Spray", C. Rode et. al.*, IEEE Trans. Magn., MAG-13, No. 1 (Jan. 1977).

"Damage to Stabilizing Materials by 400 GeV Protons", P. A. Sanger, B. P. Strauss et. al., IEEE Trans. Magn., MAG-13, No. 1 (Jan. 1977).

"Coil Extension, Deformation & Compression During Excitation in Superconducting Accelerator Dipole Magnets", A. V. Tollestrup, R. E. Peters, K. Koepke, R. H. Flora, IEEE Trans. Nucl. Sci., NS-24, No. 3 (June 1977).

"Operation of Multiple Superconducting Energy Doubler Magnets in Series", G. Kalbfleisch, P. Limon, C. Rode, IEEE Trans. Nucl. Sci., NS-24, No. 3 (June 1977).

"Energy Doubler/Saver Safety Leads", M. Kuchnir & G. Biallas, IEEE Trans. Nucl. Sci., NA-24, No. 3 (June 1977).

"Status of the Fermilab Energy Doubler/Saver Project", Energy Doubler Staff, Presented by P. V. Livdahl, IEEE Trans. Nucl. Sci., NS-24, No. 3 (June 1977).

"Magnetization Effects in Superconducting Dipole Magnets", R. E. Peters et. al.*, IEEE Trans. Nucl. Sci., NS-24, No. 3 (June 1977).

"Energy Doubler Refrigeration System", C. Rode, D. Richied, IEEE Trans. Nucl. Sci., NS-24, No. 3 (June 1977).

"Radiation Damage Limitations for the Fermilab Energy Doubler/Saver", P. A. Sanger, IEEE Trans. Nucl. Sci., NS-24, No. 3 (June 1977).

"Operation of the Fermilab Accelerator as a Proton Storage Ring", A. V. Tollestrup et. al.*, IEEE Trans. Nucl. Sci., NS-24, No. 3 (June 1977).

*Principal authors were not members of the Energy Doubler Group.

Fermilab

December 6, 1976

1976 PUBLICATIONS LIST - ENERGY DOUBLER SECTION

"A Large Scale Pumped Subcooled Liquid Helium Cooling System", P. VanderArend, S. Stoy, and D. Richied, Advances in Cryogenic Engr., 21 (1976).

"Measurement of Thermal Conductance", M. Kuchnir, Advances in Cryogenic Engr., 21, 153 (1976).

"The Fabrication of Multi-Filament NbTi Composite Wire for Accelerator Applications", B. Strauss, R. Remsbottom, and P. Reardon, Applied Polymer Symposium No. 29, (John Wiley & Sons, Inc., 1976) 53-59.

The Energy Doubler -- A Progress Report for the Energy Doubler, Saver, Collider Project, by the Superconductor Group et. al., June 1976, 2nd printing October 1976.